Pryce Christopher (Orcid ID: 0000-0002-5614-4690)

Oligodendrocyte gene expression is reduced by and influences effects of chronic social stress in mice

Flurin Cathomas[†,‡], Damiano Azzinnari[†,#], Giorgio Bergamini[†,#], Hannes Sigrist[†], Michaela Buerge[†], Vanessa Hoop[†,$], Benedikt Wicki[†], Lea Goetze[†], Sergio Soares[†], Diana Kukelova[†], Erich Seifritz[‡], Sandra Goebbels[€], Klaus-Armin Nave[€], M. Said Ghandour[6,7] , Cathal Seoighe[8], Tobias Hildebrandt[9], German Leparc[9], Holger Klein[9], Elia Stupka[9], Bastian Hengerer[10], Christopher R. Pryce[†,#,*]

[†] Preclinical Laboratory for Translational Research into Affective Disorders, Department of Psychiatry, Psychotherapy and Psychosomatics, Psychiatric Hospital, University of Zurich, Switzerland

[‡] Department of Psychiatry, Psychotherapy and Psychosomatics, Psychiatric Hospital, University of Zurich, Switzerland

[#] Neuroscience Center Zurich, University of Zurich and ETH Zurich, Switzerland

[$] ETH Zurich, Institute of Human Movement Sciences and Sport, Zurich, Switzerland

[€] Max Planck Institute of Experimental Medicine, Department of Neurogenetics, Goettingen, Germany

[6] UMR 7357, University of Strasbourg, France

[7] Department of Anatomy and Neurobiology, Virginia Commonwealth University, Richmond, VA, USA

[8] School of Mathematics, Statistics & Applied Mathematics, National University of Ireland, Galway, Ireland

[9] Target Discovery Germany, Boehringer Ingelheim Pharma GmbH & Co. KG., Biberach, Germany

[10] CNS Diseases Research Germany, Boehringer Ingelheim Pharma GmbH & Co. KG., Biberach, Germany

* Corresponding author: PLaTRAD, Department of Psychiatry, Psychotherapy & Psychosomatics, Psychiatric Hospital, University of Zurich, August Forel-Strasse 7, CH-8008 Zürich, Switzerland. E-mail: christopher.pryce@bli.uzh.ch. Tel.: +44 (0)44 634 8921.

Short title: Social stress and oligodendrocyte pathology

Date of resubmission: 18.3.2018

Abstract words: 247

Introduction words: 1155

This article has been accepted for publication and undergone full peer review but has not been through the copyediting, typesetting, pagination and proofreading process which may lead to differences between this version and the Version of Record. Please cite this article as doi: 10.1111/gbb.12475

Discussion words: 2128

Abstract

Oligodendrocyte gene expression is down-regulated in stress-related neuropsychiatric disorders, including depression. In mice, chronic social stress (CSS) leads to depression-relevant changes in brain and emotional behavior, and the present study demonstrates the involvement of oligodendrocytes in this model. In C57BL/6 (BL/6) mice, RNA-sequencing was conducted with prefrontal cortex, amygdala and hippocampus from CSS and controls; a gene enrichment database for neurons, astrocytes and oligodendrocytes was used to identify cell origin of affected genes, and cell deconvolution was applied. To assess the potential causal contribution of reduced oligodendrocyte gene expression to CSS effects, mice heterozygous for the oligodendrocyte gene cyclic nucleotide phosphodiesterase (*Cnp1*) on a BL/6 background were studied; a 2 genotype (WT, *Cnp1*$^{+/-}$) x 2 environment (control, CSS) design was used to investigate effects on emotional behaviour and amygdala microglia. In BL/6 mice, in prefrontal cortex and amygdala tissue comprising gray and white matter, CSS down-regulated expression of multiple oligodendroycte genes encoding myelin and myelin-axon-integrity proteins, and cell deconvolution identified a lower proportion of oligodendrocytes in amygdala. Quantification of oligodendrocyte proteins in amygdala gray matter did not yield evidence for reduced translation, suggesting that CSS impacts primarily on white matter oligodendrocytes or the myelin transcriptome. In *Cnp1* mice, social interaction was reduced by CSS in *Cnp1*$^{+/-}$ mice specifically; using IBA1 expression, microglia activity was increased additively by *Cnp1*$^{+/-}$ and CSS in amygdala gray and white matter. This study provides back-translational evidence that oligodendrocyte changes are relevant to the pathophysiology and potentially the treatment of stress-related neuropsychiatric disorders.

Keywords: Mouse; social stress; oligodendrocyte; differential gene expression; cell deconvolution; amygdala; gray and white matter; myelin transcriptome; myelin-axon integrity; inflammation; depression

Introduction

Chronic psychosocial stress is a major aetiological factor for some neuropsychiatric disorders including depression (Keller *et al.*, 2007; Kendler & Gardner, 2010). This 'environmental pathogen' (Caspi & Moffitt, 2006) is likely to impact on periphery and brain via various pathways, ultimately to induce changes in gene and protein expression (Arloth *et al.*, 2015; Pryce & Klaus, 2013; Tylee *et al.*, 2015). Reciprocally, allelic and epigenetic determinants of gene expression modulate stressor susceptibility (Caspi & Moffitt, 2006; Duncan & Keller, 2011; Karg *et al.*, 2011). Stress-induced psychopathologies (Cuthbert & Insel, 2013) are likely to be underlain by expression changes in specific genes and proteins within specific cell types, which in turn are localized within specific brain regions contributing to cortico-limbic circuits (Lüthi & Lüscher, 2014). Improved understanding of these stress-driven pathological pathways, including of the cell types impacted in specific regions, is essential to improve treatments.

In depression, relative to control subjects, changes in neurons (Duman & Aghajanian, 2012; Rajkowska *et al.*, 1999; Rajkowska *et al.*, 2007) and glia (Rajkowska & Miguel-Hidalgo, 2007; Rajkowska & Stockmeier, 2013) have been identified in human post-mortem brain tissue. For microglia, ionized calcium binding adaptor molecule 1 (IBA1) was increased, indicating higher microglia activation, in white matter of anterior cingulate cortex in depressed patients who committed suicide (Steiner *et al.*, 2008; Torres-Platas *et al.*, 2014). For oligodendrocytes, expression of the mature-oligodendrocyte marker myelin basic protein (MBP) was lower, indicating either fewer cells or reduced MBP expression per extant cell, in anterior frontal cortex from depressed patients (Honer *et al.*, 1999). At the transcription level, oligodendrocyte gene expression was lower in depressed patients in temporal cortex (Aston *et al.*, 2005) and amygdala (Hamidi *et al.*, 2004; Sibille *et al.*, 2009) (although see (Ding *et al.*, 2015)). Myelin thickness was reduced and expression of a number of myelination genes down-regulated in anterior cingulate cortex from probands who were depressed and had experienced early life stress (Lutz *et al.*, 2017). Myelination and myelin-axon integrity in white and gray matter are critical for efficient axonal propagation of action potentials in cortical and limbic regions of neural networks (Nave, 2010). Neuroimaging studies demonstrate that resting-state functional connectivity is altered in certain networks in depression e.g. default mode network (Grimm *et al.*, 2009; Whitfield-Gabrieli & Ford, 2012) and also that white matter integrity is compromised (Miyata *et al.*, 2016). Therefore, it is possible that stress-induced impairment of oligodendrocytes is central to the cellular pathology of depression. Further, indirect evidence for oligodendrocyte involvement in depression is provided by its high

prevalence in multiple sclerosis (Siegert & Abernethy, 2004), an autoimmune disorder characterized by oligodendrocyte pathology in white and gray matter (Calabrese *et al.*, 2015).

Animal studies of stress and oligodendrocytes are relatively few. In an important translational study, mice exposed to chronic unpredictable mild stress and depressed human subjects were compared, relative to their respective control groups, in terms of the amygdala transcriptome (Sibille *et al.*, 2009). About 30-40 genes were altered in expression in the same direction in both species; 30% of these were oligodendrocyte genes that were all down-regulated e.g. myelin basic protein (*Mbp*), myelin-associated oligodendrocyte basic protein (*Mobp*) and cyclic nucleotide phosphodiesterase (*Cnp1*) (Sibille *et al.*, 2009). Mice exposed to adult social isolation were studied in terms of prefrontal cortex myelination: expression of some myelin gene transcripts was decreased e.g. *Mbp*, *Mobp*, oligodendrocyte-specific paranodal genes *NFasc155* and *Cntn2*, as was protein expression in the case of MBP; furthermore, myelin thickness was reduced and oligodendrocyte maturation retarded (Liu *et al.*, 2012). A complementary approach to studying stress effects on oligodendrocyte gene expression is investigation of depression-relevant phenotypes in mice mutant for specific oligodendrocyte genes. For example, heterozygous expression of *Cnp1* (*Cnp1*$^{+/-}$), the gene encoding the myelin paranode protein CNP (Edgar & Sibille, 2012; Lappe-Siefke *et al.*, 2003; Lee *et al.*, 2005; Raasakka & Kursula, 2014). *Cnp1*$^{+/-}$ interacts with aging such that aged *Cnp1*$^{+/-}$ mice exhibit brain inflammation and 'catatonia-depression syndrome' comprising catatonic gripping, reduced social interest and increased fear memory (Hagemeyer *et al.*, 2012). The aged *Cnp1*$^{+/-}$ mouse demonstrates a close relationship between oligodendrocyte dysfunction, inflammation and depression therefore, with parallels to multiple sclerosis pathology (Calabrese *et al.*, 2015). Social stress also induces brain inflammation in mice, as exemplified by increased IBA1 expression in prefrontal cortex, amygdala and hippocampus (Wohleb *et al.*, 2016; Wohleb *et al.*, 2014). Stress-induced oligodendrocyte dysfunction, leading to reduced myelin-axon integrity and coincident with inflammation, could constitute an important cellular pathology in depression (Edgar & Sibille, 2012).

One stressor applied in young-adult mice is chronic social stress (CSS) (Azzinnari *et al.*, 2014; Pryce & Fuchs, 2017). Relative to controls, CSS mice exhibit depression-relevant behaviors, including reduced motivation for and learning about reward (Bergamini *et al.*, 2016; Bergamini *et al.*, in press), increased fear learning and memory (Fuertig *et al.*, 2016; Just *et al.*, in press), reduced aversion control, and increased fatigue (Azzinnari *et al.*, 2014). As determined using BOLD fMRI, CSS mice exhibit altered

resting-state functional connectivity within prefronal cortex and between prefrontal cortex-amygdala and hippocampus-amygdala, changes that are analogous to those reported for neural networks in depression (Grandjean *et al.*, 2016). CSS also induces immune activation, including increased blood levels of pro-inflammatory cytokines and blood and brain levels of kynurenines (Azzinnari *et al.*, 2014; Fuertig *et al.*, 2016).

In the present study, firstly, effects of CSS on transcriptome expression were investigated in tissue from ventromedial prefrontal cortex (vmPFC), amygdala basolateral complex (BLA) and central nucleus (CeA), and ventral hippocampus (vHIPP). The vmPFC mainly comprises myelinated pyramidal glutamate neurons (Van De Werd *et al.*, 2010). Similarly to PFC, the BLA comprises mainly myelinated principal glutamate neurons (Duvarci & Pare, 2014), whilst the CeA comprises GABA local-circuit and projection neurons. The amygdala contains two white matter tracts: the lateral external capsule, which conveys PFC inputs to amygdala, and the intermediate capsule which separates BLA and CeA (Duvarci & Pare, 2014). The vHIPP comprises the cornu ammonis subfields 2 and 3, strata of which include myelinated long-range pyramidal and trilaminar glutamate neurons. We determined whether CSS impacts on expression of genes specific to neurons, astrocytes or oligodendrocytes, using differential gene expression and cell deconvolution. CSS resulted in de-regulated gene expression in each brain region; in PFC and amygdala a substantial number of oligodendrocyte genes were down-regulated. In a second, iterative step we investigated for evidence of a causal contribution of down-regulated oligodendrocyte gene expression to the effects of CSS by studying the mutant *Cnp1* model (Hagemeyer *et al.*, 2012). Using a 2 genotype (WT, *Cnp1*$^{+/-}$) x 2 environment (control, CSS) design in young adult mice, social behaviour, fear learning-memory and microglia activity were investigated. Social interaction was reduced by CSS in *Cnp1*$^{+/-}$ mice specifically, and microglia activity was increased by *Cnp1*$^{+/-}$ and CSS additively in amygdala gray and white matter; therefore, reduced expression of one oligodendrocyte gene increases susceptibility to CSS effects. This study adds to the growing translational evidence that stress-related oligodendrocyte changes in cortico-limbic brain regions are relevant to depression pathophysiology.

Materials and Methods

Animals and housing

Four experiments were conducted with C57BL/6J male mice, and a subsequent experiment was conducted with males of a *Cnp1*-mutant C57BL/6 strain established by insertion of Cre-recombinase ORF into the *Cnp1* locus (Lappe-Siefke *et al.*, 2003). Mice were bred in-house (Zurich), the *Cnp1* mice using wildtype (WT) dams and heterozygous ($Cnp1^{+/-}$) sires (founders provided by the Max Planck Institute of Experimental Medicine, Goettingen). For each experiment, breeding pairs contributed either 1 or 2 offspring to one or both treatment groups i.e. CSS, control. Mice were weaned into littermate pairs-trios at week 3; in the *Cnp1* strain ear tissue for genotyping was taken at week 5 (Lappe-Siefke *et al.*, 2003). Mice were maintained in individually-ventilated type 2L cages at 20-22°C and 50-60% humidity under a reversed 12:12 h light-dark cycle (white lights off 07:00-19:00 h). Experimental procedures were conducted during the dark phase, at 08:00-16:00 h. Food (Complete pellet Provimi, Kliba Ltd, Kaiseraugst, Switzerland) and water were available continuously. To induce CSS the resident mice were ex-breeder males of the CD-1 strain (Janvier, Saint-Berthevin, France) aged 8 months and caged singly. The study was conducted under permits (170/2012, 149/2015) for animal experimentation issued by the Veterinary Office of canton Zürich.

Experimental design

Each of four experiments conducted with C57BL/6 mice used a different naive cohort (Fig. S1). Per experiment, mean age of CSS and control (CON) mice at study onset was 12-13 weeks (range 10-16 weeks). Experiments began with handling at study days -6/-4. This was followed at day -2 by a test of baseline motor activity (see Behavioral testing) used to counterbalance allocation of mice to CSS and CON groups. CSS and CON were conducted at days 1-15. In Expt 1 (CON n=12, CSS n=12), fresh-fixed brains were obtained at day 17 and the RNA-Seq transcriptome was measured in PFC, amygdala and HIPP tissue; data were analyzed using differential gene expression and cell deconvolution. In Expt 2 (CON n=12, CSS n=12), fresh-fixed brains were obtained again at day 17 and amygdala tissue was analyzed in RNA-Seq and differential gene expression. Based on the findings of these experiments we focused on oligodendrocyte protein expression in amygdala in Expts 3-4. In Expt 3 (CON n=12, CSS n=10), fresh-fixed brains were obtained at day 17 and western blotting was conducted for myelin proteins MBP, proteolipid protein 1 (PLP) and CNP, and for the mature-oligodendrocyte somatic protein, carbonic anhydrase II (CA II). In Expt 4 (CON n=6, CSS n=6), perfused brains were obtained at day 17 and immunoperoxidase staining was conducted for CA II and immunofluorescence staining for the

oligodendrocyte-precursor cell and mature-oligodendrocyte nuclear protein OLIG2. Expt 5 was conducted with mice of the *Cnp1* strain and used a 2 genotype (WT, *Cnp1*$^{+/-}$) x 2 environment (control, CSS) design (WT-CON n=10, WT-CSS n=11, *Cnp1*$^{+/-}$-CON n=10, *Cnp1*$^{+/-}$-CSS n=9); mean age of each group at study onset (handling, days -6/-2) was 12-13 weeks (range 10-15 weeks). CSS and CON were conducted at study days 1-15, behavioral tests of social interest and aversion learning-memory were conducted at days 16 and 17-19, respectively, and immunoperoxidase staining for the microglia protein ionized calcium-binding adapter molecule 1 (IBA 1) was conducted in amygdala in brains perfused at day 27 from the same mice now aged 16-17 weeks on average (Fig. S1).

Chronic social stress (CSS)

Mice were allocated to CSS and CON groups by counterbalancing for motor activity in Expts 1-4 and for body weight in Expt 5. CSS was conducted according to the resident-intruder protocol described in detail elsewhere (Azzinnari *et al.*, 2014; Fuertig *et al.*, 2016; Grandjean *et al.*, 2016). Briefly, on days 1-15 each CSS mouse was placed singly into the home cage of an unfamiliar aggressive CD-1 mouse, separated by a transparent, perforated plastic divider, for 24 h. In C57BL/6 mice, the CSS mouse was placed in the same compartment as the CD-1 mouse for a total of 60 s physical attack or 10 min maximum. In *Cnp1* mice, a pilot study showed that they were relatively passive during attacks and the protocol was modified: maximum 60 s physical attack on days 1-4, 40 s on days 5-10, 30 s on days 11-15, or maximum 10 min shared compartment time on any day. After the physical attack, the CSS mouse remained in the same compartment and the CD-1 mouse was transferred to the opposite compartment. The CSS x CD-1 mouse pairings were rotated so that each CSS mouse was confronted with a novel CD-1 mouse each day. In all experiments, to prevent bite wounds the lower incisors of CD-1 mice were trimmed every third day. From day 15, each CSS mouse remained in the same divided cage with the same CD-1 mouse without further attacks. Control mice remained in littermate pairs, the standard social condition in our laboratory, and were handled daily.

Region-of-interest RNA-Seq transcriptomics and differential gene expression

In Expt 1, brains were fresh frozen at day 17 and stored at -80°C. The regions of interest (ROIs) were: vmPFC focusing on infralimbic cortex and also including ventral prelimbic cortex and medial forceps minor of corpus callosum (Fig. S2A); basolateral nucleus of amygdala (BLA) also including external

capsule (EC) and intermediate capsule (IC) and some central nucleus (Fig. S2B); and vHIPP (Fig. S2C). Coronal sections (1 mm) and region-specific tissue samples were obtained as described elsewhere (Azzinnari *et al.*, 2014). Briefly, tissue (∅=1 mm) was microdissected from each hemisphere: 1x vmPFC at bregma 2.1 to 1.2 ± 0.2 mm, 1x BLA at bregma -0.7 to -1.7 ± 0.3 mm, and 2x vHIPP at bregma -2.8 to -3.9 ± 0.3 mm (Franklin, 2008). In Expt 2, the ROI in day 17 tissue was central nucleus of amygdala (CeA) also including IC (Fig. S2D). Tissue (1x ∅=0.5 mm) was microdissected from each hemisphere of a 1 mm coronal section at bregma -0.9 to -1.9 ± 0.3 mm. Bilateral biopsies were pooled, and stored at -80°C in Expt 1 and placed overnight in 10x RNAlater (Ambion) at 4°C and stored at -80°C in Expt 2. Total RNA was extracted using RNeasy Micro Kit (Qiagen) in Expt 1 and MagMax Total RNA Isolation Kit (Ambion) in Expt 2. The TrueSeq RNA Sample Preparation Kit (Illumina) was used to prepare mRNA libraries, and each was normalized to 2 nM mRNA. Libraries were sequenced using the Illumina HiSeq2000 Sequencer. Read mapping of 52 bp one direction reads to the mouse reference genome was conducted with STAR Aligner (Dobin *et al.*, 2013). Transcripts were assembled and gene expression quantified using Cuffdiff2 (Cufflinks version 2.2.0 (Trapnell *et al.*, 2013)). The criteria used for differential gene expression between CSS and CON mice were: $q < 0.05$, mean fold change > 1.30, mean reads per kilo-base per million mapped reads (RPKM) ≥ 5 in CON mice. For differentially expressed genes, the cell type of origin was identified using gene lists for enriched expression in astrocytes, neurons or oligodendrocytes available for mouse forebrain (Cahoy *et al.*, 2008).

Gene expression deconvolution

Gene expression deconvolution (GED) provides an estimate of the proportional contribution of a cell type to a heterogeneous sample (e.g. tissue) based on transcriptome data (Gaujoux & Seoighe, 2013). Using the RNA-Seq data obtained for vmPFC, amygdala and vHIPP in Expt 1, the GED digital sorting algorithm (DSA) (Zhong *et al.*, 2013) was applied to estimate relative proportions of neurons, astrocytes and oligodendrocytes. The DSA uses mean expression levels of cell type-specific genes to estimate the proportional contribution of each cell type. The genes used were those reported for astrocytes, neurons or oligodendroyctes in forebrain tissue of adult mouse (Cahoy *et al.*, 2008). For each ROI, from each enriched gene list per cell type, the 25 most enriched genes were ranked according to their mean expression in all mice. To ensure that the selected genes within each cell type had similar mean expression levels - an assumption of DSA - the 5 highest expressed genes were excluded and genes

ranked 6-15 were used for DSA analysis. The cell proportion estimates obtained were compared in CSS and CON mice using unpaired *t*-tests. To assess the specificity of DSA allocation of marker genes to the appropriate cell type, the basismarkermap function of CellMix was used (Gaujoux & Seoighe, 2013).

Western blotting for oligodendrocyte proteins

In Expt 3, brains were obtained at day 17, saline rinsed, frozen on dry ice and stored at -80°C, prior to western blotting of amygdala oligodendrocyte-myelin proteins: MBP, PLP and CNP, transcripts of which were reduced in CSS mice, and carbonic anhydrase II (CA II), a somatic marker of mature oligodendrocytes (Cerghet *et al.*, 2006; Hussain *et al.*, 2013). From a coronal section at bregma -0.8 to -1.8 mm, amygdala tissue (∅=1 mm) comprising BLA, CeA, EC and IC was microdissected bilaterally (as in Expt 1, Fig. S2B). Tissue was suspended in 80 µl ice-cold lysis buffer (50 mM Tris-HCl pH 8.0, 150 mM NaCl, 1% Triton-X-100, 0.1% SDS, 0.5% sodium deoxycholate), ground briefly and sonicated on ice for 10 s. The lysate was centrifuged (15000 g, 4°C, 10 min) and supernatant transferred to a Protein LoBind tube (Eppendorf). Total protein concentration was determined with a bicinchoninic acid (BCA) Protein Assay Kit (Pierce, Thermo Scientific). For each protein, 10 µg total protein was denatured in 1x Laemmli Buffer, 0.05M dithiothreitol, dH_2O, at 40°C for 10 min, and loaded onto a 12% SDS-polyacrylamide gel (Bio-Rad). Protein separation was performed at 200 V for 45 min, and separated proteins were transferred to nitrocellulose membranes using Trans-Blot Turbo (Bio-Rad) at 1.3 A/25 V for 7 min at RT. Membranes were washed 2x in PBS-T (1x PBS, 0.1% Tween-20) with shaking at RT for 5 min, and incubated for 1 h in blocking buffer (5% non-fat milk powder in PBS-T). Membranes were rinsed 2x 5 min in PBS-T, incubated with primary antibody at 4°C overnight, and rinsed in PBS-T for 2x 5 min. Membranes were then incubated with secondary antibody for 1 h at RT. For MBP, primary antibody was rat anti-bovine MBP (1:500; AbD Serotec) and secondary antibody was goat ECL anti-rat IgG, HRP-linked (1:2000; Amersham). For PLP, primary antibody was mouse anti-bovine PLP (1:800; AbD Serotec) and secondary was sheep ECL anti-mouse IgG, HRP-linked (1:2000; Amersham). For CNP, primary antibody was mouse anti-human CNP (1:500; Sigma) and secondary was goat anti-mouse IgG, HRP-linked (1:10000; abcam). For CA II, primary antibody was rabbit anti-rat CA II (1:2000 (Cerghet *et al.*, 2006; Hussain *et al.*, 2013)) and secondary was donkey anti-rabbit IgG, HRP-linked (1:1000; GE Healthcare). As loading control, a monoclonal HRP-linked actin-β antibody (1:100,000; Sigma) was used, run as a separate blot in the case of CNP due to similar protein sizes. After washing membranes 2x in PBS-T,

signal detection was performed with Clarity Western ECL Substrate (Bio-Rad). Band optical densities were measured using ImageJ software (NIH) and normalized relative to the band for actin-β. For MBP, the bands for the 17 and 21.5 kDa isoforms were relatively faint, and density calculations were made using the bands for the 14 and 18.5 kDa isoforms, therefore; these relative isoform intensities were consistent with the 17, 21.5 kDA and 14, 18.5 kDa isoforms being more highly expressed by developing and mature oligodendrocytes, respectively (Campagnoni, 1988).

Immunohistochemistry for carbonic anhydrase II and oligodendrocyte transcription factor 2

In Expt 4, at day 17 mice were anesthetized with pentobarbital and perfused transcardially with PBS followed by 4% paraformalaldehyde (PFA). Brains were post-fixed overnight in PFA, cryoprotected in 30% sucrose/PBS for 48 h, frozen on dry ice and stored at -80 °C. Coronal sections were cut at 25 µm, collected into microtitre well plates and stored in antifreeze solution (glucose, ethylene glycol, sodium phosphate buffer, sodium azide) at -20°C.

Immunoperoxidase staining for CA II was carried out on BLA *sensu stricto* (BLA in Fig. S2B) in two sections at bregma -1.22 to -1.34 mm. Free-floating sections were washed 2x in PBS for 5 min and quenched for 15 min in 3% H_2O_2. After washing in TBS+ (TBS 2x, 0.05% Triton) sections were placed in blocking solution (10 % horse serum, 0.3 % Triton, TBS 2x) for 1 h. Sections were then incubated with anti-CA II (1:1000; as for western blot) overnight at 4°C. Sections were washed 2x 10 min in TBS+ and incubated with goat anti-rabbit IgG (1:500, Millipore) for 1 h at RT. After 2x 10 min TBS washing, sections were incubated for 30 min with 1% avidin-biotin peroxidase complex (Vectastain ABC kit, Vector) at RT, and staining visualized with diaminobenzidine (DAB). Sections were mounted on glass slides, dried overnight, and dehydrated in ethanol and xylene. Bilateral BLA images were acquired using a brightfield microscope (Axio Observer.Z1, Zeiss) at 20x magnification. Image analysis was conducted using ImageJ and an Excel macro, with the functions thresholding, background subtraction and particle analysis. The number of CA II-positive (CA II^+) cells per BLA and % BLA area stained CA II^+, were calculated.

Immunofluorescence staining for oligodendrocyte transcription factor 2 (OLIG2) on BLA *sensu stricto* was conducted as a marker for total oligodendrocyte lineage cells including oligodendrocyte precursor cells (OPCs) and mature cells (Ehninger *et al.*, 2011). One section at bregma -1.22 was used. Free-floating sections were washed 1x in TBS+ for 10 min, placed in blocking solution (2 % donkey serum, 0.2 % Triton, TBS) for 1 h, and incubated with goat anti-human OLIG2 (1:500; R&D Systems) for

72 h at 4°C. After washing for 3x 10 min in TBS+, sections were incubated with donkey anti-goat IgG Alexa Fluor 647 (1:500; Invitrogen) for 30 min. Sections were washed 3x 10 min in TBS+ and mounted on glass slides using 1x PBS:dH_20 (1:1), and dried in a covered container prior to cover-slipping using aqueous mounting medium with DAPI (Fluoroshield, Sigma) and drying overnight. Using a confocal laser scanning microscope (SP8, Leica) equipped with a 20x objective, Z-stack images were acquired for BLA bilaterally. ImageJ software was used to analyze the maximum intensity projections of confocal z-stacks, and number of $OLIG2^+$ cells was counted using the Analyze Particles function. Parameters for intensity threshold, size exclusion and particle circularity were kept constant for all images.

Behavioral testing

Motor activity test

In Expts 1-4, using a fully-automated apparatus based on infra-red light sensors for movement detection (MultiConditioning System, TSE Systems (Cathomas *et al.*, 2015b; Pryce *et al.*, 2012)), mice were placed in an arena for a 15-min motor activity test. Scores were used to counterbalance the allocation of mice to CSS and CON groups.

Social approach test

In Expt 5, a social approach test was conducted on day 16 using a published protocol (Yang *et al.*, 2011) with an additional final stage. Briefly, the apparatus consisted of a transparent Plexiglas arena of 62.5 (L) x 41.5 (D) x 22 (H) cm, divided into three chambers of equal size, with transfer between chambers possible through openings (10 (D) x 5 (H) cm) in the dividing walls; openings could be closed by manual doors. Metal wire cups placed upside down (lower ∅=10.5 x H = 11 cm), one per outer chamber, were used to hold target mice. The test was run at 6-8 lux in a reversed light cycle room adjacent to the holding room, to which mice were transferred on the evening prior to testing. Testing was conducted at 08:00-14:00 h. Behavior was viewed remotely using a VideoMot2 system (TSE Systems) and scored semi-automatically at 1 s intervals using an Excel macro. The test comprised four 10-min phases. *Habituation to centre chamber:* Doors closed and mouse placed in centre chamber. *Habituation to all chambers*: Mouse starts in centre, all chambers empty, and doors opened; behavior scored as time spent in middle, right or left chamber, and chamber transitions. *Test of male vs object*: Mouse starts in centre, one chamber contains inverted metal cup housing an unfamiliar male and the other chamber contains an identical inverted empty metal cup (object), doors opened; behavior scored as time spent in each

chamber, time spent investigating male or object. *Test of female vs male:* Same conditions as previous stage, but with an unfamiliar estrous female housed under one cup and an unfamiliar male under the other cup. Behaviors scored and measures used were as for the previous stage. The right-left locations of empty cup, unfamiliar male/cup and unfamiliar female/cup were counter-balanced across mice/groups.

Aversion learning and memory test

The same mice were tested in an aversion learning and memory paradigm, conducted as described elsewhere (Cathomas *et al.*, 2015a). Briefly, an arena was placed on an electrified grid floor. Infrared light-beam sensors allowed for measurement of movement and its absence. The arena was placed in an attenuation chamber with light at 8 lux. An electroshock of 2 s duration and 0.2 mA current constituted the aversive unconditioned stimulus (US). The discrete conditioned stimulus (CS) consisted of a tone (6.5 kHz, 85 dB) presented for 20 s with the final 2 s contiguous with the US. The paradigm comprised three stages: *Stage 1 (day 17), motor activity and baseline freezing:* Mice were placed in the arena (context) for 15 min without CS or US. *Stage 2 (day 18), conditioning:* Mice were placed in the same context; following 300 s adaptation, mice were exposed to six CS-US pairings with an inter-trial interval (ITI) of 120 s. *Stage 3 (day 19), memory expression:* Mice were placed in the same context as stages 1 and 2. For the context expression test, mice were exposed to context without CS or US for 12 × 60 s. For the CS expression test, mice were exposed to 12 x 30 s CS separated by ITIs of 90 s. Freezing, defined as no detectable movement for at least 2 s, was calculated as % time; for analysis, mean % time spent freezing was calculated for pairs of consecutive trials. Due to technical problems reliable data could not be obtained for two mice and they were excluded from the data analysis.

Immunoperoxidase staining for ionized calcium-binding adapter molecule 1

In Expt 5, some of the same mice studied in behavioral tests (n=6 per group, selected at random) were transcardially perfused on day 27 for immunoperoxidase staining of IBA1. The methodology was similar to that described for CA II, with rabbit anti-mouse IBA1 primary antibody (1:1000; Wako) and staining visualized with DAB-Nickel (Klaus *et al.*, 2016). One section at bregma -1.22 mm was used for BLA *sensu stricto* and EC, and one section at bregma 0.74 mm for corpus callosum. In addition, one section per mouse was stained for CA II in amygdala gray matter (BLA and CeA) to assess for compensatory effects of *Cnp* heterozygosity.

Statistical analysis

Statistical analysis of behavior and immunohistochemistry data was conducted using SPSS (version 19, SPSS Inc.). Analysis of variance was conducted with between-subject factors of environment (CON, CSS) and genotype (WT, *Cnp1*$^{+/-}$), and a within-subject factor of trial for aversion learning-memory analysis. In the case of significant main or interaction effects, *post hoc* testing was conducted using the least significant difference test. Statistical significance was set at $p<0.05$. Data are presented as mean ± standard deviation (SD).

Results

CSS reduces oligodendrocyte gene expression in prefrontal cortex and amygdala

We studied CSS effects on the RNA-Seq transcriptome at day 17 for vmPFC, BLA and vHIPP (Expt 1) and CeA (Expt 2). For vmPFC (Fig. S2A), in total 47 genes met differential gene expression (DGE) crieteria: 10 genes were up-regulated and 37 were down-regulated in CSS mice; 0 of the up-regulated and 20 of the down-regulated genes were oligodendrocyte-enriched (Table 1) according to a cell-type transcriptome database for mouse forebrain tissue (Cahoy *et al.*, 2008). For BLA (Fig. S2B), in total 124 genes met the DGE criteria: 34 genes were up-regulated and 90 were down-regulated in CSS mice; 0 of the up-regulated and 12 of the down-regulated genes were oligodendrocyte-enriched (Table 2). In vHIPP (Fig. S2C), in total 136 genes met the DGE criteria: 54 genes were up-regulated and 82 were down-regulated in CSS mice; 0 of these genes were oligodendrocyte-enriched. For CeA (Fig. S2D), in total 68 genes met the DGE criteria: 23 genes were up-regulated and 45 were down-regulated in CSS mice; 0 of the up-regulated and 26 of the down-regulated genes were oligodendrocyte-enriched (Table 2).

(TABLE 1 ABOUT HERE)

(TABLE 2 ABOUT HERE)

Using the RNA-Seq data from Expt 1, gene expression deconvolution, specifically the digital sorting algorithm (DSA), was applied to estimate the proportions of astrocytes, neurons and oligodendrocytes in each ROI for CON and CSS mice. The gene lists obtained for ROI x cell-type, together with mean gene expression values, are given in Table S1. For each cell type, gene lists were similar

across the three ROIs - at least 7 of 10 genes were the same. The 5 genes with the highest expression per cell type were excluded for DSA analysis. For vmPFC and BLA, the genes excluded for oligodendrocytes, e.g. *Mobp*, *Mal*, *Mbp*, were expressed differentially in CSS and CON mice (Table 2); therefore, there was some independence between DGE and DSA analyses. As given in Table 3, for vmPFC and vHIPP there was no CSS effect on cell proportions. The mean proportion of oligodendrocytes was higher in BLA than in vmPFC and vHIPP. For BLA, the proportion of oligodendrocytes was lower in CSS than CON mice ($t(22)=-3.00$, $p<0.007$), the proportion of neurons was higher ($t(22)=2.08$, $p<0.05$) and there was no group effect on proportion of astrocytes ($p=0.91$). Indeed, each of the 10 oligodendrocyte genes used for DSA analysis (Table S1) had a lower BLA mean expression in CSS than CON mice (data not shown). As a validation step to assess the specificity of DSA assignment of marker genes to their cell type, the basismarkermap function of CellMix was applied (Gaujoux & Seoighe, 2013): assignment was most accurate for vmPFC, with 10/10 oligodendrocyte genes, 9/10 astrocyte genes and 8/10 neuron genes being correctly assigned. For BLA, again all oligodendrocyte genes were correctly assigned but only 6/10 astrocyte genes and 4/10 neuron genes (Fig. S3), and the situation was similar for vHIPP. This indicates that the marker gene lists derived from forebrain tissue (Cahoy *et al.*, 2008) were particularly accurate for vmPFC and less so for BLA and vHIPP.

Therefore, integration of RNA-Seq DGE data with a cell-type transcriptome database identified that a high number of oligodendrocyte genes were down-regulated by CSS in vmPFC, BLA and CeA tissue comprising gray and white matter. Using these vmPFC and BLA data for computational deconvolution identified a reduced contribution of oligodendrocytes to the BLA cell population in CSS mice.

(TABLE 3 ABOUT HERE)

No evidence for reduced myelin protein in gray-white matter or oligodendrocyte number in gray matter in amygdala of CSS mice

Based on the oligodendrocyte transcriptome findings for the BLA, we conducted western blotting for MBP, PLP and CNP, BLA transcripts of which were down-regulated in CSS mice, and for the mature oligodendrocyte marker CA II, the BLA transcript of which was not impacted by CSS. Brains were again collected at day 17 (Expt 3) and amygdala tissue biopsies comprised BLA, CeA, EC and IC (Fig. S2A). CSS was without effect on protein levels of MBP (Fig. 1A), PLP (Fig. 1B), CNP (Fig. 1C) and CA II (Fig. 1D). In perfused brains collected at day 17 (Expt 4), CSS effects on mature oligodendrocyte number in gray

matter of BLA and CeA were studied using CA II immunostaining. For BLA and CeA there was no CSS effect on CA II^+ cell number (Fig. 1E, F and S4A, B) or % area stained CA II^+ (Fig. 1G and S4C). A CSS effect on the total number of oligodendrocyte lineage cells in BLA gray matter was studied using OLIG2 immunofluorescence. The number of BLA $OLIG2^+$ cells was similar in CON mice (270±65) and CSS mice (237±85) (p=0.44; Fig. S5). Taken together with the lack of CSS effect on CA II^+ cells, this indicates that the generation rate of mature oligodendrocytes in BLA gray matter was unaffected by CSS.

Therefore, whilst the transcription of genes encoding MBP, PLP and CNP was reduced in BLA tissue from CSS mice, quantification of these proteins in the same gray and white matter ROI from a separate cohort did not identify a corresponding CSS effect on protein expression. Furthermore, CA II and OLIG2 did not provide evidence for a CSS effect on oligodendrocyte number and maturation in the gray matter of BLA and CeA.

(FIGURE 1 ABOUT HERE)

***Cnp1* heterozygosity influences CSS effects on emotion and microglia activation**

Whilst the methods deployed did not yield evidence for reduced translation of specific oligodendrocyte transcripts in amygdala of CSS mice, the evidence for CSS inhibition of oligodendrocyte transcription was substantial for vmPFC and amygdala. In Expt 5 we used an approach complementary to that of Expts 1-2 and investigated for a causal contribution of reduced oligodendrocyte gene expression to the effects of CSS on brain and behavior. For this we used heterozygous *Cnp1* mice: *Cnp1* was one of the oligodendrocyte genes down-regulated in the BLA in CSS mice, and when exposed to the stressor of aging $Cnp1^{+/-}$ mice exhibit 'catatonia-depression syndrome' and brain inflammation (Hagemeyer *et al.*, 2012). In young adults, a 2 genotype (WT, $Cnp1^{+/-}$) x 2 environment (control, CSS) design was used to investigate effects on emotional behavior and brain inflammation.

The social approach test was conducted at day 16. In the male versus object test, mice spent 90 ± 4 % total time in the stimulus chambers with main effects of Genotype ($p<0.007$) and Environment ($p<0.04$): $Cnp1^{+/-}$ mice spent less time in stimulus chambers than WT mice, and CSS mice spent less time there than CON mice. The ratio time in male chamber/total chamber time was 0.68 ± 0.15 (mean ± SD) and this preference for the male chamber did not differ between groups. For total investigation time (overall mean 314 ± 78 s) there was a main effect of Genotype (p=0.05), with $Cnp1^{+/-}$ mice investigating

less than WT mice. For the ratio male investigation/total investigation there was a main effect of Genotype ($p<0.02$) and a borderline interaction effect with Environment ($p=0.06$) (Fig. 2A): whilst all groups investigated the male more than the empty cup, *Cnp1*$^{+/-}$-CSS mice had a lower male investigation ratio than *Cnp1*$^{+/-}$-CON mice as well as WT-CON and WT-CSS mice. In the female versus male test, mice spent 90 $\pm$ 6 % total time in the stimulus chambers without Genotype or Environment effect. The ratio time in female chamber/total chamber time was 0.72 $\pm$ 0.13 and there was an interaction effect (Fig. 2B): within *Cnp1*$^{+/-}$ mice, CSS mice had a lower preference for the female chamber than CON mice, whilst *Cnp1*$^{+/-}$-CON mice also had a higher female preference than WT-CON mice. Underlying these ratio effects, for time in female chamber (overall mean 390 $\pm$ 72 s) there was an interaction effect ($p<0.009$) with *Cnp1*$^{+/-}$-CSS mice less in the female chamber than *Cnp1*$^{+/-}$-CON mice ($p<0.03$); for time in male chamber (153 $\pm$ 70 s) there was also an interaction effect ($p<0.03$), with *Cnp1*$^{+/-}$-CSS mice more in the male chamber than *Cnp1*$^{+/-}$-CON mice ($p<0.05$). For total investigation time there was an interaction effect (Fig. 2C) with *Cnp1*$^{+/-}$-CSS mice investigating less than *Cnp1*$^{+/-}$-CON mice. For female investigation time there was also an interaction effect (Fig. 2D) with *Cnp1*$^{+/-}$-CSS mice investigating the female less than *Cnp1*$^{+/-}$-CON mice, and also WT-CON mice investigating the female less than *Cnp1*$^{+/-}$-CON mice. The ratio female investigation/total investigation was 0.79 $\pm$ 0.11 and there was no effect of Genotype or Environment on this female preference.

(FIGURE 2 ABOUT HERE)

On day 17 the same mice were placed in a novel arena (context) to assess baseline motor activity and freezing. For total activity there was a main effect of Environment ($p<0.0001$) with CSS mice less active than CON mice. For % time spent freezing there was a main effect of Genotype ($p<0.05$) with *Cnp1*$^{+/-}$ mice (6 $\pm$ 6%) freezing less than WT mice (10 $\pm$ 6%). On day 18, mice were returned to the context for tone-shock conditioning (Fig. 3A): conditioning was indicated by acquisition of freezing across CS-US trials. There was a main effect of Environment with CSS mice freezing more than CON mice. Motor activity during shock provided a measure of pain sensitivity; there was no effect of Genotype or Environment ($p\geq0.10$). On day 19, mice were returned to the context, firstly without CS or US to test context-aversion memory (Fig. 3B): CSS mice exhibited higher freezing than CON mice and there was also a Genotype x Time interaction reflecting a more rapid decline in context memory (faster extinction)

in *Cnp1*$^{+/-}$-CON mice. This was followed by a CS-aversion memory test (Fig. 3C): there was an Environment x Trial interaction and a main effect of Environment, with CSS mice exhibiting more freezing and a slower decline in freezing (less extinction) than CON mice. This CSS effect was most pronounced in *Cnp1*$^{+/-}$ mice; a borderline Genotype main effect reflected reduced CS memory in *Cnp1*$^{+/-}$-CON mice specifically. For intervals between CS presentations (Fig. 3D) there was a main effect of Environment with CSS mice freezing more than CON mice, and a main effect of Genotype with *Cnp1*$^{+/-}$ mice freezing less than WT mice.

(FIGURE 3 ABOUT HERE)

Eight days after completion of behavioral testing, in a randomly selected subset of mice (N=6 per group), expression of the microglia marker IBA1 was assessed in BLA gray matter, EC and corpus callosum, with an increase in IBA1 positive area interpreted as microglia activation. In BLA (Fig. 4A-C) there was a main effect of Genotype with higher % IBA1^{+} area in *Cnp1*$^{+/-}$ compared with WT mice, and a borderline main effect of Environment with higher % IBA1^{+} area in CSS than CON mice. In EC (Fig. 4D) there was a main effect of Environment with higher % IBA1^{+} area in CSS than CON mice; this was particularly the case in *Cnp1*$^{+/-}$-CSS mice. In corpus callosum (Fig. 4E) there was no effect of either Genotype or Environment. Finally, to test for compensatory up-regulation of oligodendrocyte proteins in *Cnp1*$^{+/-}$ mice, CA II staining was conducted for amygdala gray matter. Indeed, compared with WT, *Cnp1*$^{+/-}$ mice had more CA II^{+} cells in BLA (Genotype main effect: $p<0.0001$; Fig. S6A-E) and CeA ($p=0.05$; Fig. S6F-K). There was no effect of CSS on AMYG CA II in this strain (Fig. S6E, K), in line with C57BL/6 mice (Fig. 1D-F).

(FIGURE 4 ABOUT HERE)

Discussion

Chronic social stress leads to reduced reward-directed behavior (Bergamini *et al.*, 2016; Bergamini *et al.*, in press), increased aversion learning, helplessness and fatigue (Azzinnari *et al.*, 2014; Fuertig *et al.*, 2016; Just *et al.*, in press), increased fMRI resting-state functional connectivity within PFC and between PFC and amygdala (Grandjean *et al.*, 2016), increased amygdala inositol levels (Grandjean *et al.*, 2016), and increased immune/inflammatory activation in periphery and amygdala and PFC (Azzinnari *et al.*,

2014; Fuertig *et al.*, 2016; Bergamini *et al.*, in press). Utilizing this depression-relevant model, the present study demonstrates that CSS in mice leads to reduced expression of a number of oligodendrocyte genes in PFC and amygdala tissue comprising gray and white matter. Furthermore, mice heterozygous for *Cnp1*, one such oligodendrocyte gene, are more sensitive to CSS in terms of reduced social interaction, whilst *Cnp1*$^{+/-}$ and CSS act additively to increase amygdala microglia activation. This study adds to the small number of rodent studies reporting stress-induced changes in oligodendrocytes and complements this with the evidence that oligodendrocyte genotype influences stress effects on depression-relevant brain-behavior states. It also provides back-translational evidence that cortico-limbic oligodendrocyte changes observed in human depression are of pathophysiological relevance.

CSS reduces oligodendrocyte gene expression in gray and white matter tissue from PFC and amygdala

Using hypothesis-free RNA-Seq we investigated CSS effects on the transcriptome in tissue from vmPFC, BLA, CeA and HIPP. In the three former regions, which each comprise gray and white matter, a high proportion of CSS-responsive genes were oligodendrocyte-enriched and all such genes were down-regulated. For mPFC this finding complements the report that chronic social isolation stress in C57BL/6 mice reduced *Mobp* and *Mbp* expression (although not *Mog*, *Mag* or *Plp1*) (Liu *et al.*, 2012). For BLA the finding complements the translational study reporting altered expression of 30-40 genes in tissue from men who had depression and BALB/c mice exposed to chronic unpredictable mild stress (CUMS) (Sibille *et al.*, 2009); eight of these were oligodendrocyte genes and their expression was always down-regulated, including *Mbp*, *Mobp*, *Bcas1*, *Pllp* and *Cnp1* which were down-regulated in CSS mice in the present study. The CeA was even more responsive to CSS in terms of the number of down-regulated oligodendrocyte genes, including most of the genes that were down-regulated in BLA and vmPFC. Comparison of the findings for BLA (EC, BLA, IC, CeA) and CeA (IC, CeA) suggests that CeA oligodendrocytes are more sensitive to CSS; the IC white matter tract, which contains axon projections to GABA neurons in medial intercalated cell masses (Duvarci & Pare, 2014), might be particularly stress sensitive. This variation between ROIs concurs with the proposal that oligodendrocyte function, including gene expression levels, varies between brain regions (Ornelas *et al.*, 2016).

Genes down-regulated by CSS in amygdala and mPFC encode proteins for synthesis, maintenance and compaction of myelin, e.g. *Mal, Mbp, Mobp*, as well as proteins for maintenance of

myelin-axon stability at paranodes and nodes of Ranvier, e.g. *Cnp1*, *Mag*. Interestingly, the genes impacted by CSS demonstrate remarkable overlap with the genes recently reported to constitute the 'myelin transcriptome', that is, genes the mRNA for which is not only localized in oligodendrocytes but also in myelin (Thakurela *et al.*, 2016). This would suggest that CSS might be acting to inhibit myelin transcript trafficking to or survival at myelin sheath assembly sites, rather than or in addition to oligodendrocyte cell-body transcription of myelin genes. Should stress-induced reduction of myelin gene transcription – in cell bodies and/or myelin - result in reduced translation of myelin proteins, a key candidate pathology would be compromised myelin-axon integrity at paranodes and nodes (Edgar & Sibille, 2012; Matute *et al.*, 2013). In indirect support of this, the gene with the highest fold-change between CSS and CON mice in amygdala was sodium channel type IV beta (*Scn4b*), which was down-regulated in CSS mice by 2.46-fold in BLA and 1.73-fold in CeA. Voltage-gated sodium-channel subunits, including IV beta, are concentrated in nodes of Ranvier and axon initial segments of axons, and modulate sodium-channel activity and propagation of axon potentials (Catterall, 2000; Miyazaki *et al.*, 2014). Evidence for altered axonal function in CSS mice is provided by increased resting state functional connectivity between amygdala and each of PFC, cingulate cortex and vHIPP (Grandjean *et al.*, 2016). Expression changes in neuronal ion-channel subunit genes have been reported for depression (Smolin *et al.*, 2012). Further examples of genes down-regulated in CSS mice and encoding proteins related to myelin-axon function were potassium channel, subfamily K, member 2 (*Kcnk2*), down-regulated 1.5-fold in BLA from CSS mice, and adenosine A2a receptor (*Adora2a*), highly (but not specifically) expressed in oligodendrocytes (Melani *et al.*, 2009) and down-regulated 1.9-fold in BLA from CSS mice.

As well as facilitating identification of the cellular origin of CSS-responsive genes, the cell-enriched gene lists for mouse forebrain tissue (Cahoy *et al.*, 2008) were also used to conduct gene expression deconvolution (GED). To date GED has been applied primarily to immune system RNA-Seq data (Gaujoux & Seoighe, 2013) and to our knowledge this is a first application to brain data. In BLA there was a 2 % reduction in contribution of oligodendrocytes in CSS relative to CON mice; given that the estimated contribution of oligodendrocytes to the BLA total cell population was 11 %, this constitutes an approximate 20 % decrease in the oligodendrocyte proportion in the BLA of CSS mice, which is substantial. In terms of protein-level evidence for CSS effects on oligodendrocytes, given the DGE and GED findings we focused on the BLA. Using the same gray and white matter ROI as for RNA-Seq there was no effect of CSS on expression of MBP, PLP or CNP, each of which exhibited reduced transcript

in CSS mice. Within gray matter, i.e. BLA *sensu stricto*, there was no CSS effect on number of mature oligodendrocytes using CA II and also no effect on number of oligodendrocyte lineage cells using OLIG2; these findings suggest a lack of CSS effect on the generation of new mature oligodendrocytes in BLA gray matter. To our knowledge the only rodent study to date that reports on stress-induced reduction of oligodendrocyte protein levels is that of chronic isolation stress leading to reduced MBP in mPFC using western blot (Liu *et al.*, 2012). Also, myelin sheaths around axons in mPFC gray matter were thinner (hypomyelination) in these mice, based on electron microscopy (Liu *et al.*, 2012). A future CSS study will need to apply such ultrastructural analysis in gray and white matter regions of amygdala and mPFC. Given the overlap between the identities of CSS-impacted oligodendrocyte transcripts in this study and those comprising the myelin transcriptome (Thakurela *et al.*, 2016), it is possible that CSS-impacted protein levels were also restricted to myelin translation and were thus not identified by our tissue-level analysis. Future study will need to focus on purified myelin samples.

Reduced *Cnp1* influences CSS effects on emotional behavior and microglia activation in amygdala gray and white matter

To investigate for evidence of a causal contribution of down-regulated oligodendrocyte gene expression to the psycho-neuro-immune effects of CSS, we studied a *Cnp1* mutant mouse. Consistent with the function of CNP1 in maintaining paranodal myelin-axon integrity (Edgar & Sibille, 2012; Snaidero *et al.*, 2017), from young adulthood *Cnp1* homozygous-mutant ($Cnp1^{-/-}$) mice exhibit universal axonal swellings and neurodegeneration in the absence of myelin changes (Lappe-Siefke *et al.*, 2003). This contrasts with, for example, $Mbp^{-/-}$ mice, which do exhibit hypomyelination (Klugmann *et al.*, 1997; Readhead *et al.*, 1987). $Cnp1^{-/-}$ mice react to minor brain insult with increased axon degeneration, astrogliosis and microgliosis, demonstrating that "oligodendrocyte dysfunctions can trigger a vicious cycle of neurodegeneration and low-grade inflammation amplified by nonspecific activators of the innate immune system." (Wieser *et al.*, 2013). Heterozygous *Cnp1* mice also exhibit increased susceptibility to neuroinflammation, but only with a second risk factor, for example aging: 24-month $Cnp1^{+/-}$ mice exhibit 'catatonia-depression syndrome' comprising persistent catatonic gripping, reduced social interest and increased conditioned aversion memory (Hagemeyer *et al.*, 2012). This behavioral state co-occurs with brain inflammation in white and gray matter in the form of more $IBA1^{+}$ cells, Mac-3^{+} microglia, astrocytes ($GFAP^{+}$), infiltrating T-lymphocytes (CD3), and axonal swelling. In contrast, in

young-adult *Cnp1*$^{+/-}$ mice, as used in the present study, these markers are unchanged relative to WT (Hagemeyer *et al.*, 2012).

With respect to behavior, in the social approach test *Cnp1*$^{+/-}$-CSS mice exhibited a deficit in social interaction with male and female C57BL/6 mice. Reduced interest in BL/6 mice is of particular significance given that aggressors used for CSS were CD-1 mice; such a generalized reduction in social behavior has been reported only rarely for social stress, e.g. (Berton *et al.*, 2006). In the test of aversion learning and memory, as expected (Fuertig *et al.*, 2016; Just *et al.*, in press) CSS led to higher acquisition of tone freezing; this CSS-induced increase in fear was similar in *Cnp1*$^{+/-}$ and WT mice. With regard to fear memory, *Cnp1*$^{+/-}$-CON mice expressed less freezing than WT-CON mice, suggesting compromised memory function in amygdala and hippocampus in mice with deficient *Cnp1* (Duvarci & Pare, 2014; Xu *et al.*, 2016). Despite this, *Cnp1*$^{+/-}$-CSS mice expressed high and similar freezing to that of WT-CSS mice, such that the net CSS effect on aversion salience was greater in *Cnp1*$^{+/-}$ mice. Therefore, reduced *Cnp1* renders mice more sensitive to CSS in terms of reduced salience of social/sexual stimuli and high memory of aversive stimuli. Interestingly, *Cnp* $^{-/-}$ (homozygous) mice actually exhibit reduced emotional reactivity to aversive stimuli relative to WT (Edgar *et al.*, 2011); furthermore, when exposed to CUMS, *Cnp1*$^{-/-}$-CUMS mice are less reactive to aversive stimuli than WT-CUMS mice. These findings suggest that full *Cnp1* knockout leads to compensatory changes in the oligodendrocyte transcriptome and, indeed, several oligodendrocyte genes e.g. *Mbp*, *Mobp* and *Cldn11*, were up-regulated in the BLA of *Cnp1*$^{-/-}$ relative to WT mice (to a similar extent in CUMS and control mice) (Edgar *et al.*, 2011). These same genes were down-regulated in the BLA by CUMS in BALB/c mice (Sibille *et al.*, 2009) and by CSS in C57BL/6 mice in the present study. Also with regard to compensation, the *Cnp*$^{+/-}$ mice had more CA II^{+} cells in amygdala than did WT, and this might reflect processes that somewhat attenuated the sensitivity of *Cnp*$^{+/-}$ mice to CSS effects.

There was an additive effect of *Cnp1*$^{+/-}$ and CSS in terms of increased microglia activity based on IBA1 expression. This was the case for BLA gray matter and the EC white matter tract, although not for corpus callosum. Therefore, a candidate pathogenesis for the behavioral phenoytpes of *Cnp1*$^{+/-}$-CSS mice is reduced paranodal myelin-axon integrity associated with increased inflammation. This would be consistent with the findings in *Cnp1*$^{+/-}$ aged mice (Hagemeyer *et al.*, 2012). Furthermore, in C57BL/6 mice, CSS leads to activation of the inflammation-dependent kynurenine pathway in mPFC, amygdala and HIPP, whilst pharmacological reversal of kynurenine-pathway hyperactivity normalizes aversion

memory in CSS mice (Fuertig *et al.*, 2016). CSS also increases in vivo amygdala levels of inositol, which could reflect increased inflammation and/or altered myelin-axon integrity (Grandjean *et al.*, 2016). The current findings suggest that oligodendrocytes contribute to these effects, in line with the evidence that oligodendrocytes are both sensitive to and contribute to stress states, including inflammation, oxidative stress and excitotoxicity (Calabrese *et al.*, 2015; Matute *et al.*, 2013).

Study limitations and summary

As noted above, it will be important in a subsequent study to increase the resolution at which CSS effects on oligodendrocyte genes and proteins are analyzed. This will require ultrastructural protein analysis using electron microscopy, as applied in a study of stress effects on myelin thickness (Liu *et al.*, 2012), and should include myelination, myelin-axon integrity at paranodal regions and nodes, and axon status. It will be important to study gray matter and white matter sub-regions, as demonstrated in mouse models for multiple sclerosis (Calabrese *et al.*, 2015). Indeed, the availability of transgenic mice with labeled oligodendrocytes e.g. (Cahoy *et al.*, 2008; Deng *et al.*, 2014) will allow for analysis of stress effects on transcriptome and proteome in pure oligodendrocyte samples. Finally, it will be important to assess CSS effects on the myelin transcriptome (Thakurela *et al.*, 2016).

Chronic social stress in mice leads to depression-relevant changes in emotional behavior, brain functional connectivity and immune activation in periphery and brain, and this study demonstrates that it also reduces expression of oligodendrocyte genes in mPFC and amygdala tissue comprising gray and white matter. Furthermore, a genotype of reduced *Cnp1* expression leads to a CSS effect of attenuated interest in social/sexual stimuli and acts additively with CSS to increase microglia activation in amygdala. These findings add to the rodent model evidence that compromised oligodendrocyte function is an important component of stress-induced brain-behavior changes, and provide back-translational evidence that the cortico-limbic oligodendrocyte changes observed in depression are relevant to its pathogenesis and therefore potentially its treatment.

REFERENCES

Arloth, J., Bogdan, R., Weber, P., Frishman, G., Menke, A., Wagner, K.V., Balsevich, G., Schmidt, M.V., Karbalai, N., Czamara, D., Altmann, A., Trumbach, D., Wurst, W., Mehta, D., Uhr, M., Klengel, T., Erhardt, A., Carey, C.E., Conley, E.D., Ruepp, A., Muller-Myhsok, B., Hariri, A.R. & Binder, E.B. (2015) Genetic Differences in the Immediate Transcriptome Response to Stress Predict Risk-Related Brain Function and Psychiatric Disorders. *Neuron,* **86,** 1189-1202.

Aston, C., Jiang, L. & Sokolov, B.P. (2005) Transcriptional profiling reveals evidence for signaling and oligodendroglial abnormalities in the temporal cortex from patients with major depressive disorder. *Mol Psychiatry,* **10,** 309-322.

Azzinnari, D., Sigrist, H., Staehli, S., Palme, R., Hildebrandt, T., Leparc, G., Hengerer, B., Seifritz, E. & Pryce, C.R. (2014) Mouse social stress induces increased fear conditioning, helplessness and fatigue to physical challenge together with markers of altered immune and dopamine function. *Neuropharmacology,* **85,** 328-341.

Bergamini, G., Cathomas, F., Auer, S., Sigrist, H., Seifritz, E., Patterson, M., Gabriel, C. & Pryce, C.R. (2016) Mouse psychosocial stress reduces motivation and cognitive function in operant reward tests: A model for reward pathology with effects of agomelatine. *Eur Neuropsychopharmacol,* **26,** 1448-1464.

Bergamini, G., Mechtersheimer, J., Azzinnari, D., Sigrist, H., Buerge, M., Dallmann, R., Freije, R., Seifritz, E., Ferger, B., Suter, T. & Pryce, C.R. (in press) Chronic social stress induces peripheral and central immune activation, blunted mesolimbic dopamine function, and reduced reward-directed behaviour. *Neurobiology of Stress*.

Berton, O., McClung, C.A., Dileone, R.J., Krishnan, V., Renthal, W., Russo, S.J., Graham, D., Tsankova, N.M., Bolanos, C.A., Rios, M., Monteggia, L.M., Self, D.W. & Nestler, E.J. (2006) Essential role of BDNF in the mesolimbic dopamine pathway in social defeat stress. *Science,* **311,** 864-868.

Cahoy, J.D., Emery, B., Kaushal, A., Foo, L.C., Zamanian, J.L., Christopherson, K.S., Xing, Y., Lubischer, J.L., Krieg, P.A., Krupenko, S.A., Thompson, W.J. & Barres, B.A. (2008) A transcriptome database for astrocytes, neurons, and oligodendrocytes: a new resource for understanding brain development and function. *J Neurosci,* **28,** 264-278.

Calabrese, M., Magliozzi, R., Ciccarelli, O., Geurts, J.J., Reynolds, R. & Martin, R. (2015) Exploring the origins of grey matter damage in multiple sclerosis. *Nat Rev Neurosci,* **16,** 147-158.

Campagnoni, A.T. (1988) Molecular biology of myelin proteins from the central nervous system. *Journal of neurochemistry,* **51,** 1-14.

Caspi, A. & Moffitt, T.E. (2006) Gene-environment interactions in psychiatry: joining forces with neuroscience. *Nat Rev Neurosci,* **7,** 583-590.

Cathomas, F., Fuertig, R., Sigrist, H., Newman, G.N., Hoop, V., Bizzozzero, M., Mueller, A., Luippold, A., Ceci, A., Hengerer, B., Seifritz, E., Fontana, A. & Pryce, C.R. (2015a) CD40-TNF activation in mice induces extended sickness behavior syndrome co-incident with but not dependent on activation of the kynurenine pathway. *Brain Behav Immun,* **50,** 125-140.

Cathomas, F., Stegen, M., Sigrist, H., Schmid, L., Seifritz, E., Gassmann, M., Bettler, B. & Pryce, C.R. (2015b) Altered emotionality and neuronal excitability in mice lacking KCTD12, an auxillary subunit of GABAB receptors associated with mood disorders. *Translational Psychiatry,* **5:e510. doi: 10.1038/tp.2015.8.**

Catterall, W.A. (2000) Structure and regulation of voltage-gated Ca2+ channels. *Annu Rev Cell Dev Biol,* **16,** 521-555.

Cerghet, M., Skoff, R.P., Bessert, D., Zhang, Z., Mullins, C. & Ghandour, M.S. (2006) Proliferation and death of oligodendrocytes and myelin proteins are differentially regulated in male and female rodents. *J Neurosci,* **26,** 1439-1447.

Cuthbert, B.N. & Insel, T.R. (2013) Toward the future of psychiatric diagnosis: the seven pillars of RDoC. *BMC Med,* **11,** 1741-7015.

Deng, Y., Kim, B., He, X., Kim, S., Lu, C., Wang, H., Cho, S.G., Hou, Y., Li, J., Zhao, X. & Lu, Q.R. (2014) Direct visualization of membrane architecture of myelinating cells in transgenic mice expressing membrane-anchored EGFP. *Genesis,* **52,** 341-349.

Ding, Y., Chang, L.-C., Wang, X., Guilloux, J.-P., Parrish, J., Oh, H., French, B.J., Lewis, D.A.T., G.C & Sibille, E. (2015) Molecular and genetic characterization of depression: overlap with other psychiatric disorders and aging. *Molecular Neuropsychiatry,* **1,** 1-12.

Dobin, A., Davis, C.A., Schlesinger, F., Drenkow, J., Zaleski, C., Jha, S., Batut, P., Chaisson, M. & Gingeras, T.R. (2013) STAR: ultrafast universal RNA-seq aligner. *Bioinformatics,* **29,** 15-21.

Duman, R.S. & Aghajanian, G.K. (2012) Synaptic dysfunction in depression: potential therapeutic targets. *Science,* **338,** 68-72.

Duncan, L.E. & Keller, M.C. (2011) A critical review of the first 10 years of candidate gene-by-environment interaction research in psychiatry. *The American journal of psychiatry,* **168,** 1041-1049.

Duvarci, S. & Pare, D. (2014) Amygdala microcircuits controlling learned fear. *Neuron,* **82,** 966-980.

Edgar, N. & Sibille, E. (2012) A putative functional role for oligodendrocytes in mood regulation. *Transl Psychiatry,* **1,** 34.

Edgar, N.M., Touma, C., Palme, R. & Sibille, E. (2011) Resilient emotionality and molecular compensation in mice lacking the oligodendrocyte-specific gene Cnp1. *Transl Psychiatry,* **20,** 40.

Ehninger, D., Wang, L.P., Klempin, F., Romer, B., Kettenmann, H. & Kempermann, G. (2011) Enriched environment and physical activity reduce microglia and influence the fate of NG2 cells in the amygdala of adult mice. *Cell and Tissue Research,* **345,** 69-86.

Franklin, K.B.J., Paxinos, G (2008) The Mouse Brain: In Stereotaxic Coordinates. Elsevier, Amsterdam.

Fuertig, R., Azzinnari, D., Bergamini, G., Cathomas, F., Sigrist, H., Seifritz, E., Vavassori, S., Luippold, A., Hengerer, B., Ceci, A. & Pryce, C.R. (2016) Mouse chronic social stress increases blood and brain kynurenine pathway activity and fear behaviour: Both effects are reversed by inhibition of indoleamine 2,3-dioxygenase. *Brain Behav Immun,* **54,** 59-72.

Gaujoux, R. & Seoighe, C. (2013) CellMix: a comprehensive toolbox for gene expression deconvolution. *Bioinformatics,* **29,** 2211-2212.

Grandjean, J., Azzinnari, D., Seuwen, A., Sigrist, H., Seifritz, E., Pryce, C.R. & Rudin, M. (2016) Chronic psychosocial stress in mice leads to changes in brain functional connectivity and metabolite levels comparable to human depression. *Neuroimage,* **142,** 544-552.

Grimm, S., Boesiger, P., Beck, J., Schuepbach, D., Bermpohl, F., Walter, M., Ernst, J., Hell, D., Boeker, H. & Northoff, G. (2009) Altered negative BOLD responses in the default-mode network during emotion processing in depressed subjects. *Neuropsychopharmacol,* **34,** 932-943.

Hagemeyer, N., Goebbels, S., Papiol, S., Kastner, A., Hofer, S., Begemann, M., Gerwig, U.C., Boretius, S., Wieser, G.L., Ronnenberg, A., Gurvich, A., Heckers, S.H., Frahm, J., Nave, K.A. & Ehrenreich, H. (2012) A myelin gene causative of a catatonia-depression syndrome upon aging. *EMBO Mol Med,* **4,** 528-539.

Hamidi, M., Drevets, W.C. & Price, J.L. (2004) Glial reduction in amygdala in major depressive disorder is due to oligodendrocytes. *Biol Psychiatry,* **55,** 563-569.

Honer, W.G., Falkai, P., Chen, C., Arango, V., Mann, J.J. & Dwork, A.J. (1999) Synaptic and plasticity-associated proteins in anterior frontal cortex in severe mental illness. *Neuroscience,* **91,** 1247-1255.

Hussain, R., Ghoumari, A.M., Bielecki, B., Steibel, J., Boehm, N., Liere, P., Macklin, W.B., Kumar, N., Habert, R., Mhaouty-Kodja, S., Tronche, F., Sitruk-Ware, R., Schumacher, M. & Ghandour, M.S. (2013) The neural androgen receptor: a therapeutic target for myelin repair in chronic demyelination. *Brain,* **136,** 132-146.

Just, S., Chenard, B.L., Ceci, A., Strassmeier, T., Chong, J.A., Blair, N.T., Gallaschun, R.J., del Camino, D., Cantin, S., D'Amours, M., Eickmeier, C., Fanger, C.M., Hecker, C., Hessler, D.P., Hengerer, B., Kroker, K.S., Malekiani, S., Mihalek, R., McLaughlin, J., Rast, G., Witek, J., Sauer, A., Pryce, C.R. & Moran, M.M. (in press) Pharmacological inhibition of TRPC4 and TRPC5 with HC-070 ameliorates behaviors associated with anxiety and depression in mice. *PLoS one*.

Karg, K., Burmeister, M., Shedden, K. & Sen, S. (2011) The serotonin transporter promoter variant (5-HTTLPR), stress, and depression meta-analysis revisited: evidence of genetic moderation. *Arch Gen Psychiatry,* **68,** 444-454.

Keller, M.C., Neale, M.C. & Kendler, K.S. (2007) Association of different adverse life events with distinct patterns of depressive symptoms. *The American journal of psychiatry,* **164,** 1521-1529.

Kendler, K.S. & Gardner, C.O. (2010) Dependent stressful life events and prior depressive episodes in the prediction of major depression: the problem of causal inference in psychiatric epidemiology. *Arch Gen Psychiatry,* **67,** 1120-1127.

Klaus, F., Paterna, J.C., Marzorati, E., Sigrist, H., Gotze, L., Schwendener, S., Bergamini, G., Jehli, E., Azzinnari, D., Fuertig, R., Fontana, A., Seifritz, E. & Pryce, C.R. (2016) Differential effects of peripheral and brain tumor necrosis factor on inflammation, sickness, emotional behavior and memory in mice. *Brain Behav Immun,* **58,** 310-326.

Klugmann, M., Schwab, M.H., Puhlhofer, A., Schneider, A., Zimmermann, F., Griffiths, I.R. & Nave, K.A. (1997) Assembly of CNS myelin in the absence of proteolipid protein. *Neuron,* **18,** 59-70.

Lappe-Siefke, C., Goebbels, S., Gravel, M., Nicksch, E., Lee, J., Braun, P.E., Griffiths, I.R. & Nave, K.A. (2003) Disruption of Cnp1 uncouples oligodendroglial functions in axonal support and myelination. *Nat Genet,* **33,** 366-374.

Lee, J., Gravel, M., Zhang, R., Thibault, P. & Braun, P.E. (2005) Process outgrowth in oligodendrocytes is mediated by CNP, a novel microtubule assembly myelin protein. *J Cell Biol,* **170,** 661-673.

Liu, J., Dietz, K., DeLoyht, J.M., Pedre, X., Kelkar, D., Kaur, J., Vialou, V., Lobo, M.K., Dietz, D.M., Nestler, E.J., Dupree, J. & Casaccia, P. (2012) Impaired adult myelination in the prefrontal cortex of socially isolated mice. *Nature Neuroscience,* **15,** 1621-1623.

Lüthi, A. & Lüscher, C. (2014) Pathological circuit function underlying addiction and anxiety disorders. *Nature Neuroscience,* **17,** 1635-1643.

Lutz, P.E., Tanti, A., Gasecka, A., Barnett-Burns, S., Kim, J.J., Zhou, Y., Chen, G.G., Wakid, M., Shaw, M., Almeida, D., Chay, M.A., Yang, J., Lariviere, V., M'Boutchou, M.N., van Kempen, L.C., Yerko, V., Prud'homme, J., Davoli, M.A., Vaillancourt, K., Theroux, J.F., Bramoulle, A., Zhang, T.Y., Meaney, M.J., Ernst, C., Cote, D., Mechawar, N. & Turecki, G. (2017) Association of a History of Child Abuse With Impaired Myelination in the Anterior Cingulate Cortex: Convergent Epigenetic, Transcriptional, and Morphological Evidence. *The American journal of psychiatry,* **174,** 1185-1194.

Matute, C., Domercq, M., Perez-Samartin, A. & Ransom, B.R. (2013) Protecting white matter from stroke injury. *Stroke,* **44,** 1204-1211.

Melani, A., Cipriani, S., Vannucchi, M.G., Nosi, D., Donati, C., Bruni, P., Giovannini, M.G. & Pedata, F. (2009) Selective adenosine A2a receptor antagonism reduces JNK activation in oligodendrocytes after cerebral ischaemia. *Brain,* **132,** 1480-1495.

Miyata, S., Taniguchi, M., Koyama, Y., Shimizu, S., Tanaka, T., Yasuno, F., Yamamoto, A., Iida, H., Kudo, T., Katayama, T. & Tohyama, M. (2016) Association between chronic stress-induced structural abnormalities in Ranvier nodes and reduced oligodendrocyte activity in major depression. *Scientific reports,* **6,** 23084.

Miyazaki, H., Oyama, F., Inoue, R., Aosaki, T., Abe, T., Kiyonari, H., Kino, Y., Kurosawa, M., Shimizu, J., Ogiwara, I., Yamakawa, K., Koshimizu, Y., Fujiyama, F., Kaneko, T., Shimizu, H., Nagatomo, K., Yamada, K., Shimogori, T., Hattori, N., Miura, M. & Nukina, N. (2014) Singular localization of sodium channel beta4 subunit in unmyelinated fibres and its role in the striatum. *Nat Commun,* **5**.

Nave, K.-A. (2010) Myelination and support of axonal integrity by glia. *Nature,* **468,** 244-252.

Ornelas, I.M., McLane, L.E., Saliu, A., Evangelou, A.V., Khandker, L. & Wood, T.L. (2016) Heterogeneity in oligodendroglia: Is it relevant to mouse models and human disease? *J Neurosci Res,* **94,** 1421-1433.

Pryce, C.R., Azzinnari, D., Sigrist, H., Gschwind, T., Lesch, K.-P. & Seifritz, E. (2012) Establishing a learned helplessness effect paradigm in C57BL/6 mice: behavioural evidence for emotional, motivational and cognitive effects of aversive uncontrollability per se. *Neuropharmacol,* **62,** 358-372.

Pryce, C.R. & Fuchs, E. (2017) Chronic psychosocial stressors in adulthood: Studies in mice, rats and tree shrews. *Neurobiol Stress,* **6,** 94-103.

Pryce, C.R. & Klaus, F. (2013) Translating the evidence for gene association with depression into mouse models of depression-relevant behaviour: current limitations and future potential. *Neurosci Biobehav Rev,* **37,** 1380-1402.

Raasakka, A. & Kursula, P. (2014) The myelin membrane-associated enzyme 2',3'-cyclic nucleotide 3'-phosphodiesterase: on a highway to structure and function. *Neurosci Bull,* **30,** 956-966.

Rajkowska, G. & Miguel-Hidalgo, J.J. (2007) Gliogenesis and glial pathology in depression. *CNS Neurol Disord Drug Targets,* **6,** 219-233.

Rajkowska, G., Miguel-Hidalgo, J.J., Wei, J., Dilley, G., Pittman, S.D., Meltzer, H.Y., Overholser, J.C., Roth, B.L. & Stockmeier, C.A. (1999) Morphometric evidence for neuronal and glial prefrontal cell pathology in major depression. *Biol Psychiatry,* **45,** 1085-1098.

Rajkowska, G., O'Dwyer, G., Teleki, Z., Stockmeier, C.A. & Miguel-Hidalgo, J.J. (2007) GABAergic neurons immunoreactive for calcium binding proteins are reduced in the prefrontal cortex in major depression. *Neuropsychopharmacology,* **32,** 471-482.

Rajkowska, G. & Stockmeier, C.A. (2013) Astrocyte pathology in major depressive disorder: insights from human postmortem brain tissue. *Curr Drug Targets,* **14,** 1225-1236.

Readhead, C., Popko, B., Takahashi, N., Shine, H.D., Saavedra, R.A., Sidman, R.L. & Hood, L. (1987) Expression of a myelin basic protein gene in transgenic shiverer mice: correction of the dysmyelinating phenotype. *Cell,* **48,** 703-712.

Sibille, E., Wang, Y., Joeyen-Waldorf, J., Gaiteri, C., Surget, A., Oh, S., Belzung, C., Tseng, G.C. & Lewis, D.A. (2009) A molecular signature of depression in the amygdala. *The American journal of psychiatry,* **166,** 1011-1024.

Siegert, R.J. & Abernethy, D.A. (2004) Depression in multiple sclerosis: a review. *Journal of Neurology, Neurosurgery and Psychiatry,* **76,** 469-475.

Smolin, B., Karry, R., Gal-Ben-Ari, S. & Ben-Shachar, D. (2012) Differential expression of genes encoding neuronal ion-channel subunits in major depression, bipolar disorder and schizophrenia: implications for pathophysiology. *Int J Neuropsychopharmacol,* **15,** 869-882.

Snaidero, N., Velte, C., Myllykoski, M., Raasakka, A., Ignatev, A., Werner, H.B., Erwig, M.S., Mobius, W., Kursula, P., Nave, K.A. & Simons, M. (2017) Antagonistic Functions of MBP and CNP Establish Cytosolic Channels in CNS Myelin. *Cell Rep,* **18,** 314-323.

Steiner, J., Bielau, H., Brisch, R., Danos, P., Ullrich, O., Mawrin, C., Bernstein, H.G. & Bogerts, B. (2008) Immunological aspects in the neurobiology of suicide: elevated microglial density in schizophrenia and depression is associated with suicide. *J Psychiatr Res,* **42,** 151-157.

Thakurela, S., Garding, A., Jung, R.B., Muller, C., Goebbels, S., White, R., Werner, H.B. & Tiwari, V.K. (2016) The transcriptome of mouse central nervous system myelin. *Scientific reports,* **6,** 25828.

Torres-Platas, S.G., Cruceanu, C., Chen, G.G., Turecki, G. & Mechawar, N. (2014) Evidence for increased microglial priming and macrophage recruitment in the dorsal anterior cingulate white matter of depressed suicides. *Brain Behav Immun,* **42,** 50-59.

Trapnell, C., Hendrickson, D.G., Sauvageau, M., Goff, L., Rinn, J.L. & Pachter, L. (2013) Differential analysis of gene regulation at transcript resolution with RNA-seq. *Nature Biotechnology,* **31,** 46-53.

Tylee, D.S., Chandler, S.D., Nievergelt, C.M., Liu, X., Pazol, J., Woelk, C.H., Lohr, J.B., Kremen, W.S., Baker, D.G., Glatt, S.J. & Tsuang, M.T. (2015) Blood-based gene-expression biomarkers of post-traumatic stress disorder among deployed marines: A pilot study. *Psychoneuroendocrinology,* **51,** 472-494.

Van De Werd, H.J., Rajkowska, G., Evers, P. & Uylings, H.B. (2010) Cytoarchitectonic and chemoarchitectonic characterization of the prefrontal cortical areas in the mouse. *Brain Struct Funct,* **214,** 339-353.

Whitfield-Gabrieli, S. & Ford, J.M. (2012) Default mode network activity and connectivity in psychopathology. *Annual Review of Clinical Psychology,* **8,** 49-76.

Wieser, G.L., Gerwig, U.C., Adamcio, B., Barrette, B., Nave, K.A., Ehrenreich, H. & Goebbels, S. (2013) Neuroinflammation in white matter tracts of Cnp1 mutant mice amplified by a minor brain injury. *Glia,* **61,** 869-880.

Wohleb, E.S., Franklin, T., Iwata, M. & Duman, R.S. (2016) Integrating neuroimmune systems in the neurobiology of depression. *Nat Rev Neurosci,* **17,** 497-511.

Wohleb, E.S., Patterson, J.M., Sharma, V., Quan, N., Godbout, J.P. & Sheridan, J.F. (2014) Knockdown of interleukin-1 receptor type-1 on endothelial cells attenuated stress-induced neuroinflammation and prevented anxiety-like behavior. *J Neurosci,* **34,** 2583-2591.

Xu, C., Krabbe, S., Grundemann, J., Botta, P., Fadok, J.P., Osakada, F., Saur, D., Grewe, B.F., Schnitzer, M.J., Callaway, E.M. & Luthi, A. (2016) Distinct Hippocampal Pathways Mediate Dissociable Roles of Context in Memory Retrieval. *Cell,* **167,** 961-972 e916.

Yang, M., Silverman, J.L. & Crawley, J.N. (2011) Automated three-chambered social approach task for mice. *Curr Protoc Neurosci,* **8**.

Zhong, Y., Wan, Y.W., Pang, K., Chow, L.M. & Liu, Z. (2013) Digital sorting of complex tissues for cell type-specific gene expression profiles. *BMC Bioinformatics,* **14,** 1471-2105.

Acknowledgements

We are grateful to Björn Henz and Alex Osei for animal care, and to Werner Rust, Ulli Bode, Georg Wieser, Ursina Nüesch and Stefano Vavassori for expert technical assistance. This research was funded by the Swiss National Science Foundation (grant 31003A_160147 to C.R.P.), the German Research Foundation (grant SPP 1757 to S.G.), and a collaboration between Boehringer Ingelheim Pharma GmbH & Co. KG, Germany and PLaTRAD, University of Zurich, Switzerland. Tobias Hildebrandt, German Leparc, Holger Klein, Elia Stupka and Bastian Hengerer are employees of Boehringer Ingelheim Pharma GmbH & Co. KG, Germany. The other authors declare no conflict of interest.

Figure legends

Figure 1. Western blot and immunohistochemistry findings for oligodendrocyte proteins in basolateral amygdala of CSS and CON C57BL/6 mice at day 17 (Experiments 3 and 4). (A)-(D) Western blot analysis of target proteins normalized to actin-β in BLA gray and white matter. Values of CSS (N=10) and CON (N=12) mice are calculated relative to the mean value of CON mice (set to 1.0) and error bars are SD: (A) Myelin basic protein; the graph depicts relative MBP densities calculated using the 18 kDa isoform, and there was a similar absence of CSS effect using the 14 kDa isoform. (B) Proteolipid protein (myelin) 1. (C) Cyclic nucleotide phosphodiesterase. (D) Carbonic anhydrase II. (E)-(G) Immunoperoxidase staining for CA II in BLA gray matter at day 17. CON (N=6) and CSS (N=6) values are mean + SD: (E) Representative photomicrographs from CON and CSS mice. Scale bar = 50 µm. (F) Total number of CA II-positive cells. (G) Percent area covered by CA II-positive staining. All *p* values were obtained in unpaired t-tests.

Figure 2. Genotype (WT, *Cnp1*$^{+/-}$) x Environment (CON, CSS) effects on behavior in a three-chamber social approach test at day 16 in *Cnp1*-mutant mice on a C57BL/6 background (Experiment 5). (A) Proportion of total investigation time spent with the male in the male versus object phase. (B) Proportion of total chamber time spent in the estrous female chamber in the female versus male phase. (C) Total investigation time in the female versus male phase. (D) Female investigation time in the female versus male phase. Values are mean + SD, WT-CON N=10, WT-CSS N=11, *Cnp1*$^{+/-}$-CON N=10, *Cnp1*$^{+/-}$-CSS N=9. p values are for 2 x 2 full-factorial ANOVA and the least significant difference test for post hoc pairwise comparisons.

Figure 3. Genotype (WT, *Cnp1*$^{+/-}$) x Environment (CON, CSS) effects on freezing behavior in an aversion conditioning and memory test at days 18 and 19 in *Cnp1*-mutant mice on a C57BL/6 background (Experiment 5). Conditioning at day 18: (A) Left panel: Mean % time freezing during presentation of a tone stimulus (18 s CS followed by 2 s CS + 0.2 mA footshock US) in blocks of 2 consecutive CS-US trials. Right panel: Overall mean + SD % time freezing during all 6 CS-US trials. Memory expression at day 19: (B) Left panel: Mean % time freezing to the context (no CS or US) in blocks of 2 min. Right panel: Overall mean + SD % time freezing to the context during all 12 min. (C) Left panel: Mean % time freezing to 30-s CS in blocks of 2 consecutive CS trials. Right panel: Overall mean + SD % time freezing during all 12 CS trials. (D) Left panel: Mean % time freezing during the 90-s inter-trial intervals in blocks of 2 intervals.

Right panel: Overall mean + SD % time freezing during all 12 intervals. WT-CON N=10, WT-CSS N=10, *Cnp1*$^{+/-}$-CON N=9, *Cnp1*$^{+/-}$-CSS N=9. p values are for full-factorial ANOVA and the least significant difference test for post hoc pairwise comparisons.

Figure 4. Genotype (WT, *Cnp1*$^{+/-}$) x Environment (CON, CSS) effects on microglia activity using IBA1 immunoperoxidase staining at day 27 in *Cnp1*-mutant mice on a C57BL/6 background (Experiment 5). (A)-(B) Representative micrographs from (A) WT-CON mouse and (B) *Cnp1*$^{+/-}$-CSS mouse, showing characteristic IBA1 staining in BLA gray matter. Scale bar = 50 µm. (C) Percent area of IBA1-positive staining in BLA gray matter. (D) Percent area of IBA1-positive staining in external capsule of amygdala. (E) Percent area of IBA1-positive staining in corpus callosum. Values are mean + SD, N=6 per group. p values are for 2 x 2 full-factorial ANOVA and the least significant difference test for post hoc pairwise comparisons: a vs b $p<0.05$.

Figure 1

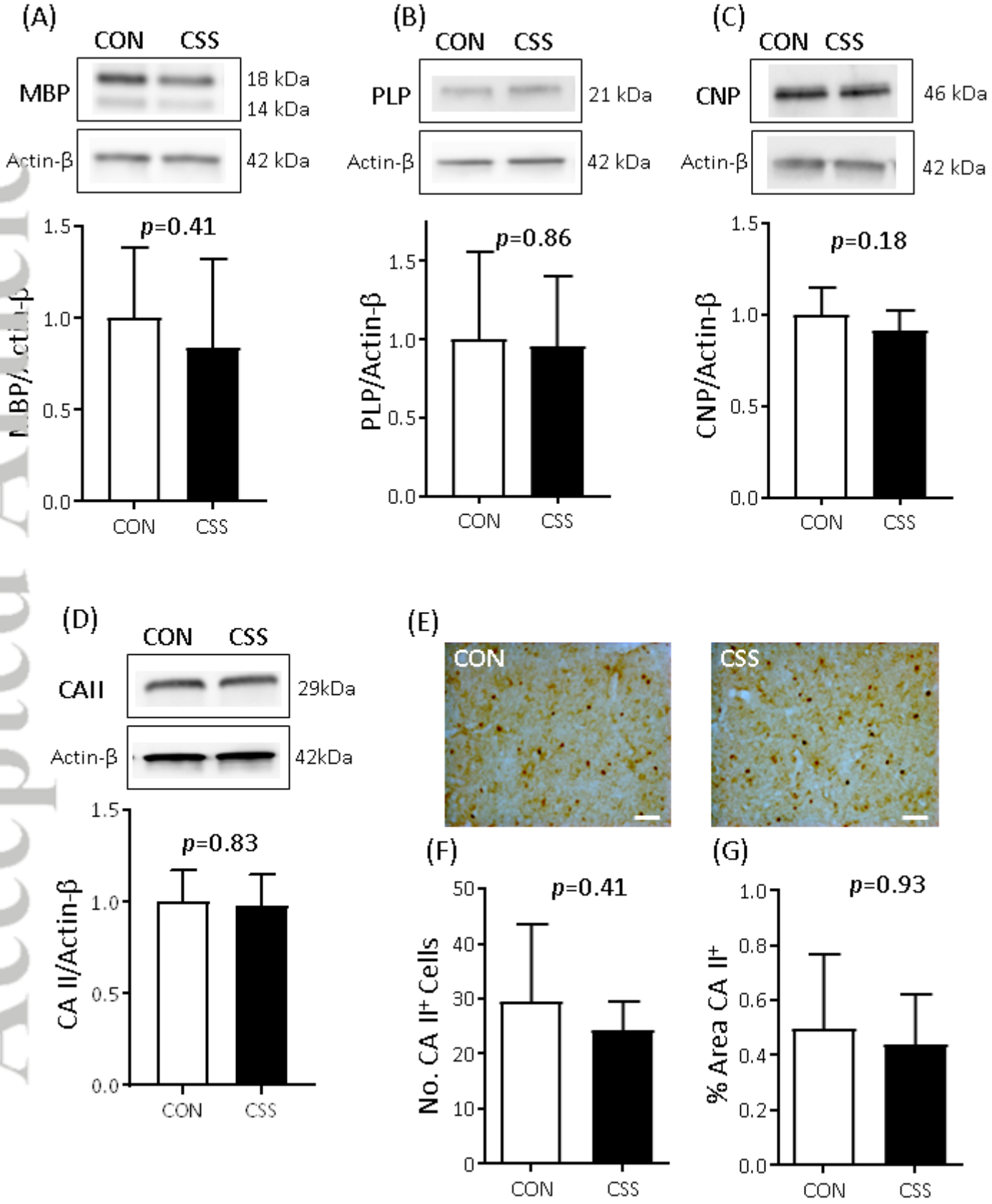

Figure 2

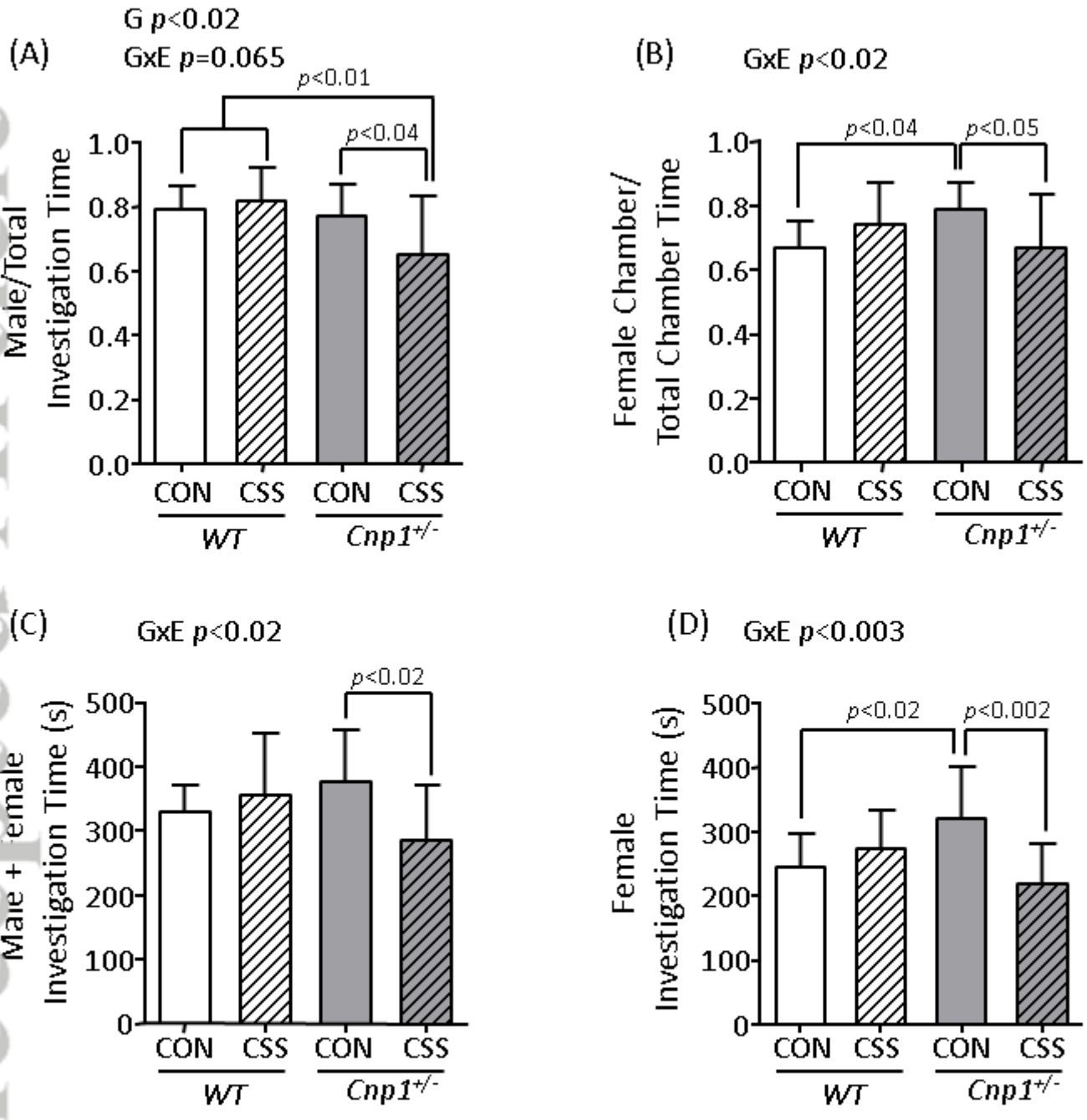

Figure 3

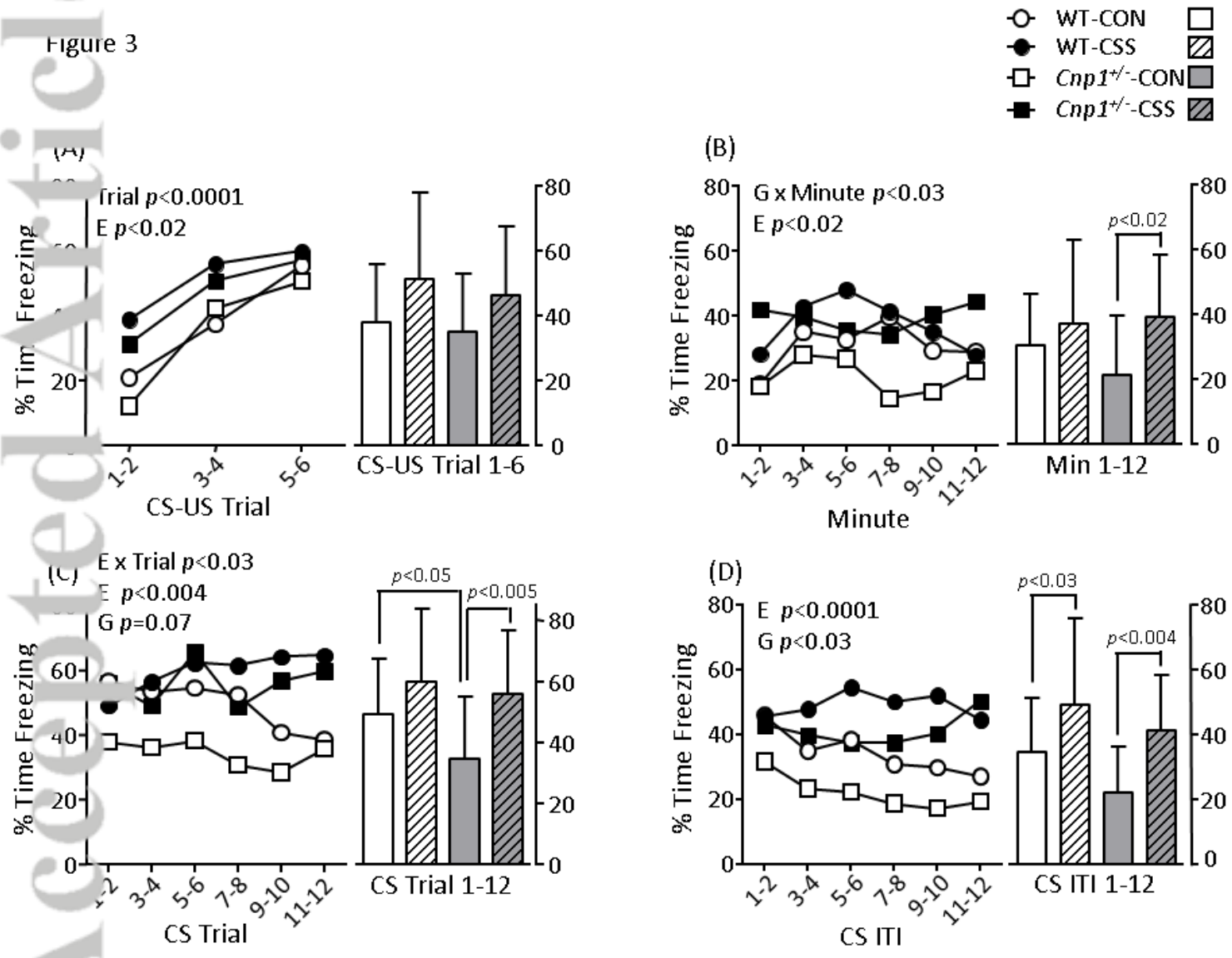

Figure 4

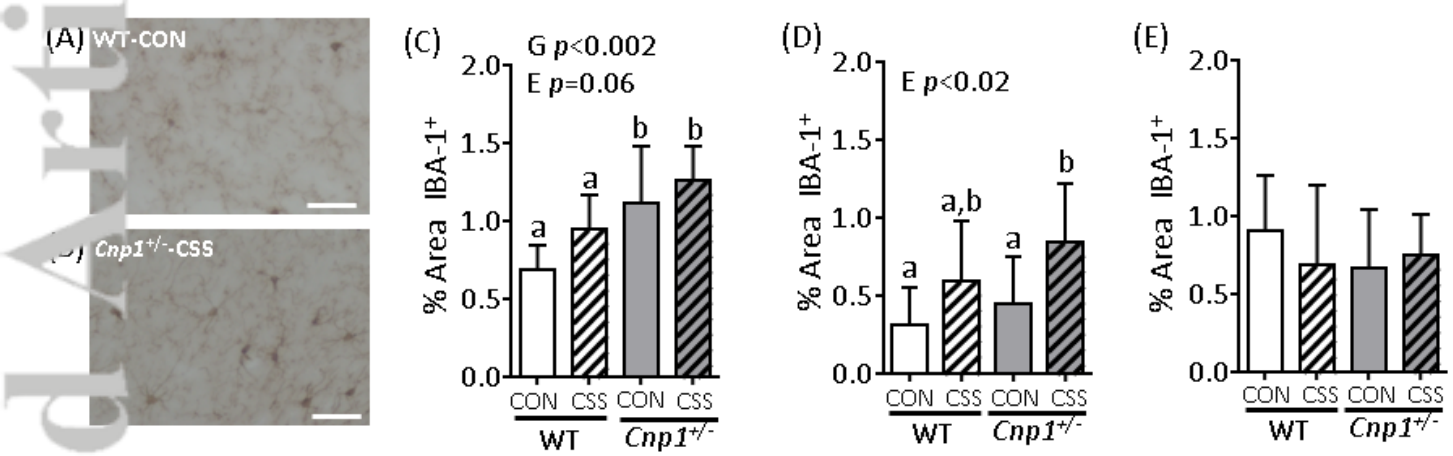

Figure 4

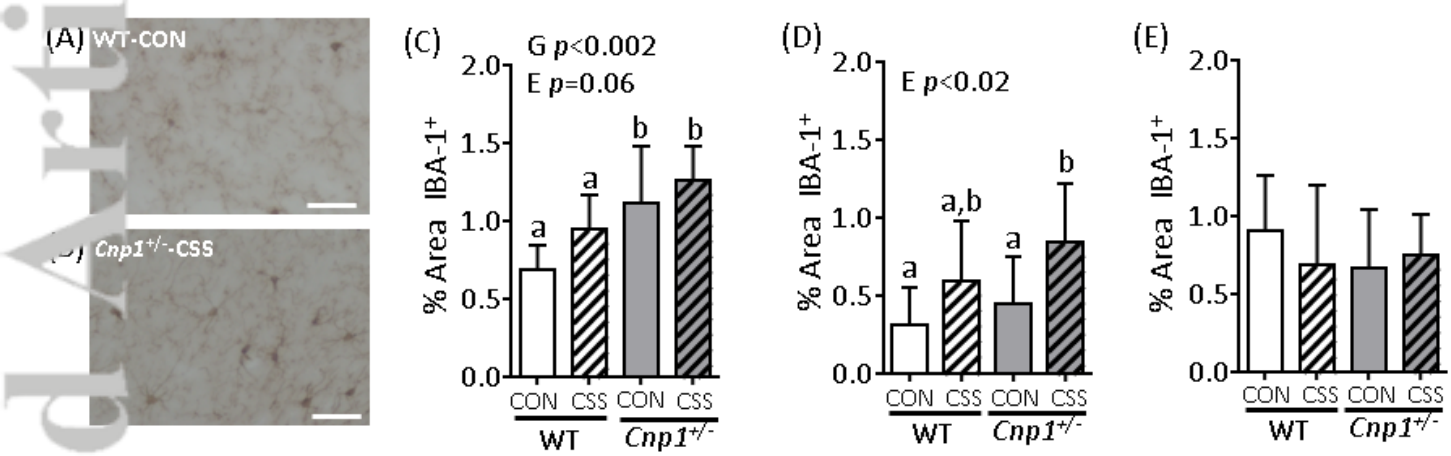

Slide1.TIF

Figure 4

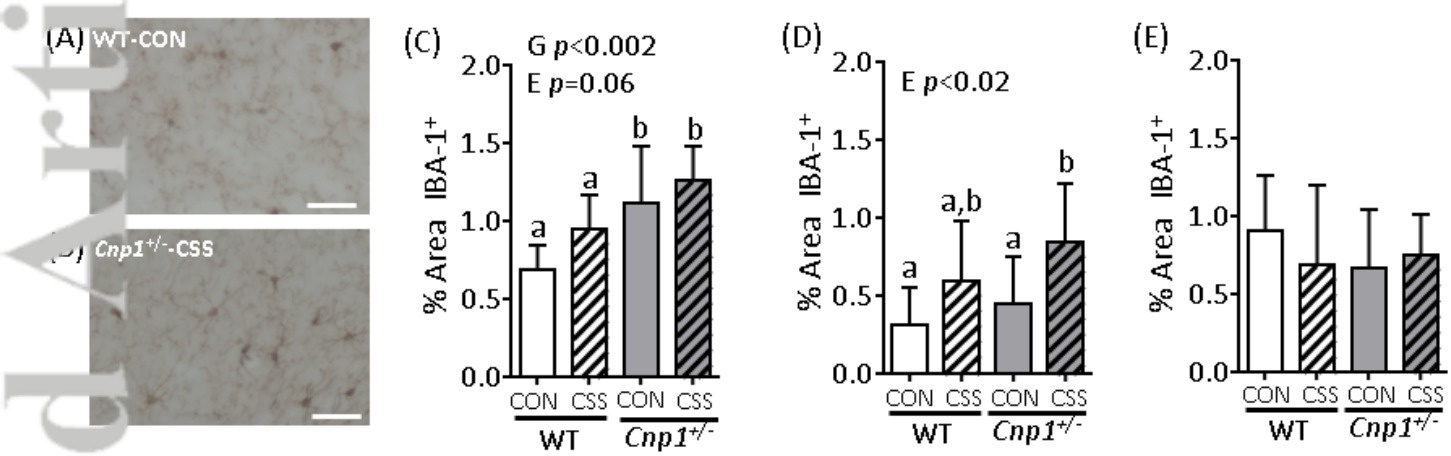

Slide1.TIF

Figure 4

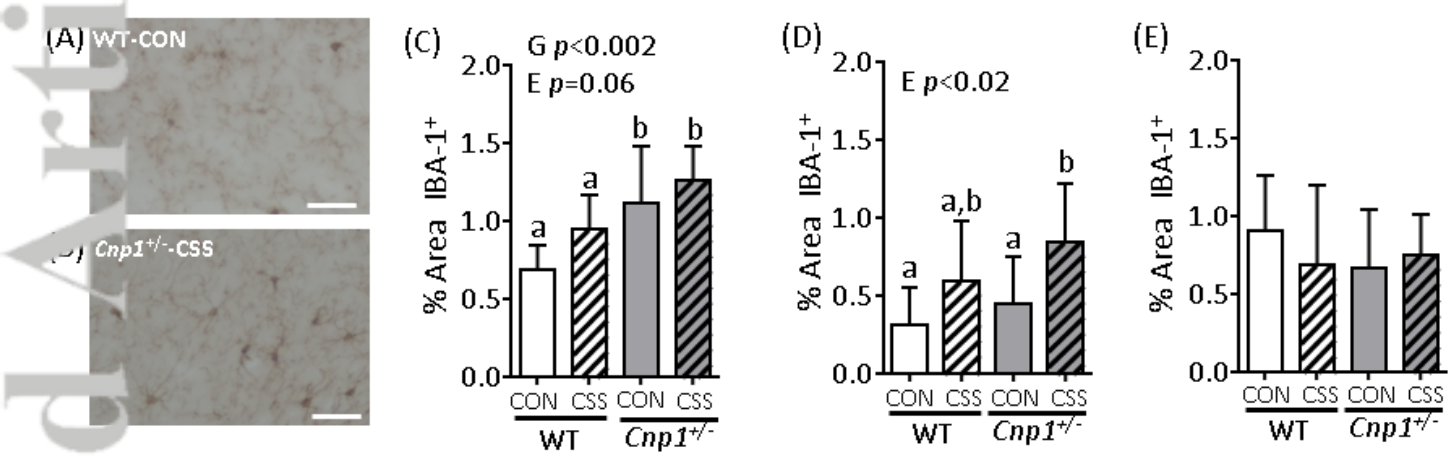

Slide1.TIF

Figure 4

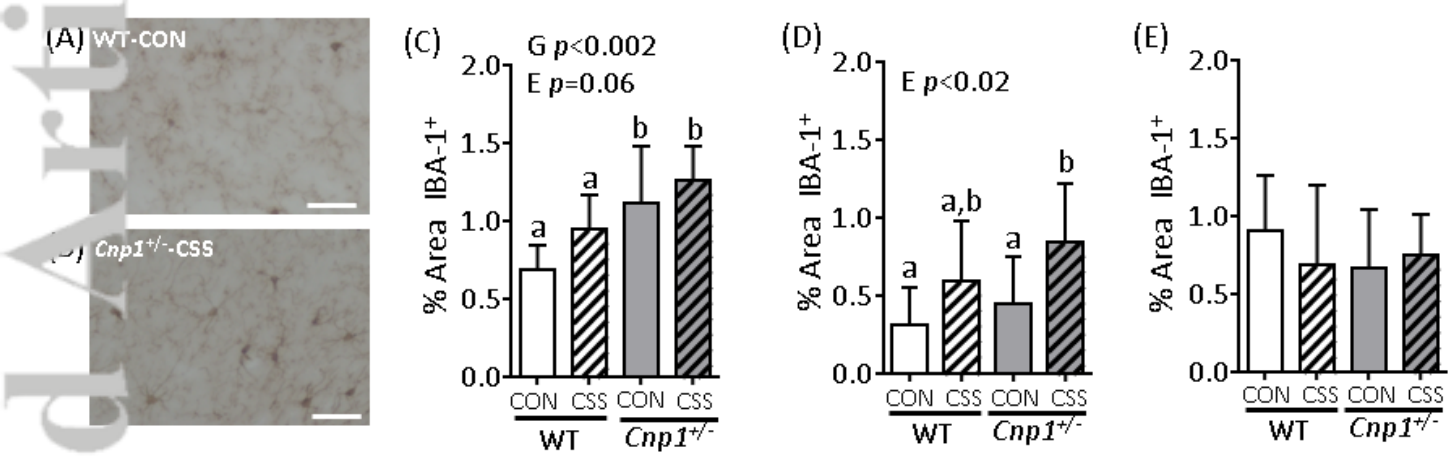

Slide1.TIF

Table 1. Oligodendrocyte genes exhibiting differential gene expression in CSS and control mice in ventro-medial prefrontal cortex (vmPFC) tissue

vmPFC (IL + PrL + CC), CON n=12, CSS n=12

Gene	RPKM CON	RPKM CSS	Fold Change	*q*-value
Opalin	8	5	1.54↓	0.01
Mal	91	61	1.49↓	0.02
Mobp	254	172	1.48↓	0.03
Aspa	10	7	1.44↓	0.03
Bcas1	50	35	1.42↓	0.02
Gjc2	7	5	1.42↓	0.02
Mag	50	36	1.39↓	0.02
Gm98	10	7	1.38↓	0.02
Ttyh2	9	7	1.36↓	0.02
Tmem88b	16	12	1.36↓	0.02
Gjc3	12	9	1.35↓	0.02
Cldn11	71	53	1.34↓	0.02
Mog	30	22	1.34↓	0.03
Plxnb3	5	3	1.34↓	0.03
Gpr37	16	12	1.34↓	0.02
Fa2h	26	12	1.33↓	0.02
Gatm	42	32	1.33↓	0.02
Tspan2	37	28	1.31↓	0.02
Pllp	19	14	1.30↓	0.02
Sox10	17	13	1.30↓	0.02
Car2	81	63	1.27↓	0.02
Cnp1	117	86	1.37↓	0.55

Candidate genes were derived from 80 oligodendrocyte-specific genes according to Cahoy et al. (2008, Supplemental Table S5).
Genes were then included if (i) $q < 0.05$, (ii) control RPKM > 5 and (iii) fold change > 1.3.
IL, infralimbic cortex; PrL, prelimbic cortex, CC, corpus callosum
Cnp1 values are given because Expt 5 was conducted with a *Cnp1* transgenic strain.
Car2 values are given because CA II expression was studied in Expts 3-5.

Table 2. Oligodendrocyte genes exhibiting differential gene expression in CSS and control mice in amygdala tissue

BLA (BLA + EC + IC + CeA), CON n=12, CSS n=12

Gene	RPKM CON	RPKM CSS	Fold Change	*q*-value
Opalin	6	4	1.60↓	0.003
Mal	66	45	1.44↓	0.003
Mobp	182	127	1.43↓	0.003
Mag	36	26	1.38↓	0.003
Tmem88b	12	9	1.36↓	0.003
Mbp	756	558	1.35↓	0.003
Cldn11	51	38	1.33↓	0.003
Bcas1	37	28	1.31↓	0.003
Pllp	16	12	1.30↓	0.003
Trf	70	52	1.34↓	0.007
Plp1	378	288	1.31↓	0.009
Cnp1	92	70	1.33↓	0.02
Car2	84	82	1.00	0.99

CeA (CeA + IC), CON n=12, CSS n=12

Gene	RPKM CON	RPKM CSS	Fold Change	*q*-value
Cldn11	134	88	1.53↓	0.01
Mog	67	44	1.52↓	0.01
Opalin	17	11	1.52↓	0.01
Anln	16	10	1.50↓	0.01
Mbp	1558	1046	1.49↓	0.01
Gjb1	11	7	1.49↓	0.02
Plekhh1	10	7	1.48↓	0.01
Mal	153	103	1.48↓	0.01
Mag	65	44	1.47↓	0.01
Mobp	499	341	1.46↓	0.01
Aspa	23	16	1.46↓	0.01
Ermn	43	30	1.45↓	0.01
Tmem88b	37	25	1.44↓	0.01
Adamts4	6	4	1.43↓	0.01
Bcas1	97	67	1.42↓	0.01
Pllp	27	19	1.40↓	0.01
Pmp22	16	11	1.40↓	0.01
Gjc3	25	18	1.40↓	0.01
Tspan2	64	46	1.39↓	0.01
Sept4	211	154	1.37↓	0.01
Gatm	78	57	1.37↓	0.01
Ugt8a	33	24	1.36↓	0.01
Fa2h	28	21	1.36↓	0.01
Gm98	15	11	1.36↓	0.01
Gpr37	23	17	1.36↓	0.01
Lgi3	27	20	1.33↓	0.01
Car2	182	162	1.12↓	0.07
Cnp1	182	131	1.39↓	0.10

Candidate genes were derived from 80 oligodendrocyte-specific genes according to Cahoy et al. (2008, Supplemental Table S5).
Genes were then included if (i) $q < 0.05$, (ii) control RPKM > 5 and (iii) fold change > 1.3. Expt 1, genes n=12; Expt 2, genes n=26.
Cnp1 values are given for Expt 2 because Expt 5 was conducted with a *Cnp1* transgenic strain.
Car2 values are given because CA II expression was studied in Expts 3-5.
BLA, basolateral amygdala; EC, external capsule; IC, intermediate capsule; CeA, central nucleus of amygdala

Table 3. Region of interest cell-type percentages estimated using the digital sorting algorithm (DSA)

	CON (n=12)	CSS (n=12)	*t*-test
vmPFC (IL + PrL + CC)			
Astrocytes	12.57 ± 2.93	12.49 ± 3.28	$p = 0.95$
Neurons	83.80 ± 6.14	84.75 ± 4.87	$p = 0.67$
Oligodendrocytes	3.63 ± 3.74	2.76 ± 1.83	$p = 0.47$
BLA (BLA + EC + IC + CeA)			
Astrocytes	22.55 ± 2.09	22.45 ± 2.41	$p = 0.91$
Neurons	65.77 ± 2.94	68.27 ± 3.18	$p < 0.05$
Oligodendrocytes	11.68 ± 2.30	9.28 ± 1.67	$p < 0.007$
vHIPP (CA2 + CA3)			
Astrocytes	31.88 ± 5.26	34.20 ± 3.91	$p = 0.22$
Neurons	62.10 ± 4.18	60.24 ± 3.20	$p = 0.22$
Oligodendrocytes	6.02 ± 2.03	5.56 ± 2.06	$p = 0.57$

Values are mean ± SD.
Genes used for DSA are given in Table S1, and were derived from the RNA-Seq expression data obtained in Expt 1 and the cell type-specific enriched gene listed for mouse forebrain (Cahoy et al, 2008).
vmPFC, ventro-medial prefrontal cortex; IL, infralimbic cortex; PrL, prelimbic cortex; CC, corpus callosum; BLA, basolateral amygdala; EC, external capsule; IC, intermediate capsule; CeA, central nucleus of amygdala; vHIPP, ventral hippocampus; CA2, cornu ammonis 2; CA3, cornu ammonis 3.